Electronic Supplementary Material (ESI) for New Journal of Chemistry.

Insights into the levulinate-based ionic liquid class: synthesis, cellulose dissolution evaluation and ecotoxicity assessment

Andrea Mezzetta, [a] Stefano Becherini, [a] Carlo Pretti, [b,c] Gianfranca Monni, [c] Valentina Casu, [c] Cinzia Chiappe [a] and Lorenzo Guazzelli *[a]

Supporting Information

Table of contents

[a] A. Mezzetta, S. Becherini, C. Chiappe, L. Guazzelli
Department of Pharmacy
University of Pisa
Via Bonanno 6, Pisa (Italy)
*E-mail: lorenzo.guazzelli@unipi.it

[b] C. Pretti
Department of Veterinary Sciences,
University of Pisa,
Via Livornese lato monte, San Piero a Grado (PI) 56122, Pisa, Italy

[c] C. Pretti, G. Monni, V. Casu
Interuniversity Consortium of Marine Biology of Leghorn "G. Bacci", Livorno, 57128, Italy

Fig S1. ^{1}H NMR of **EMIMLev** at 25 °C

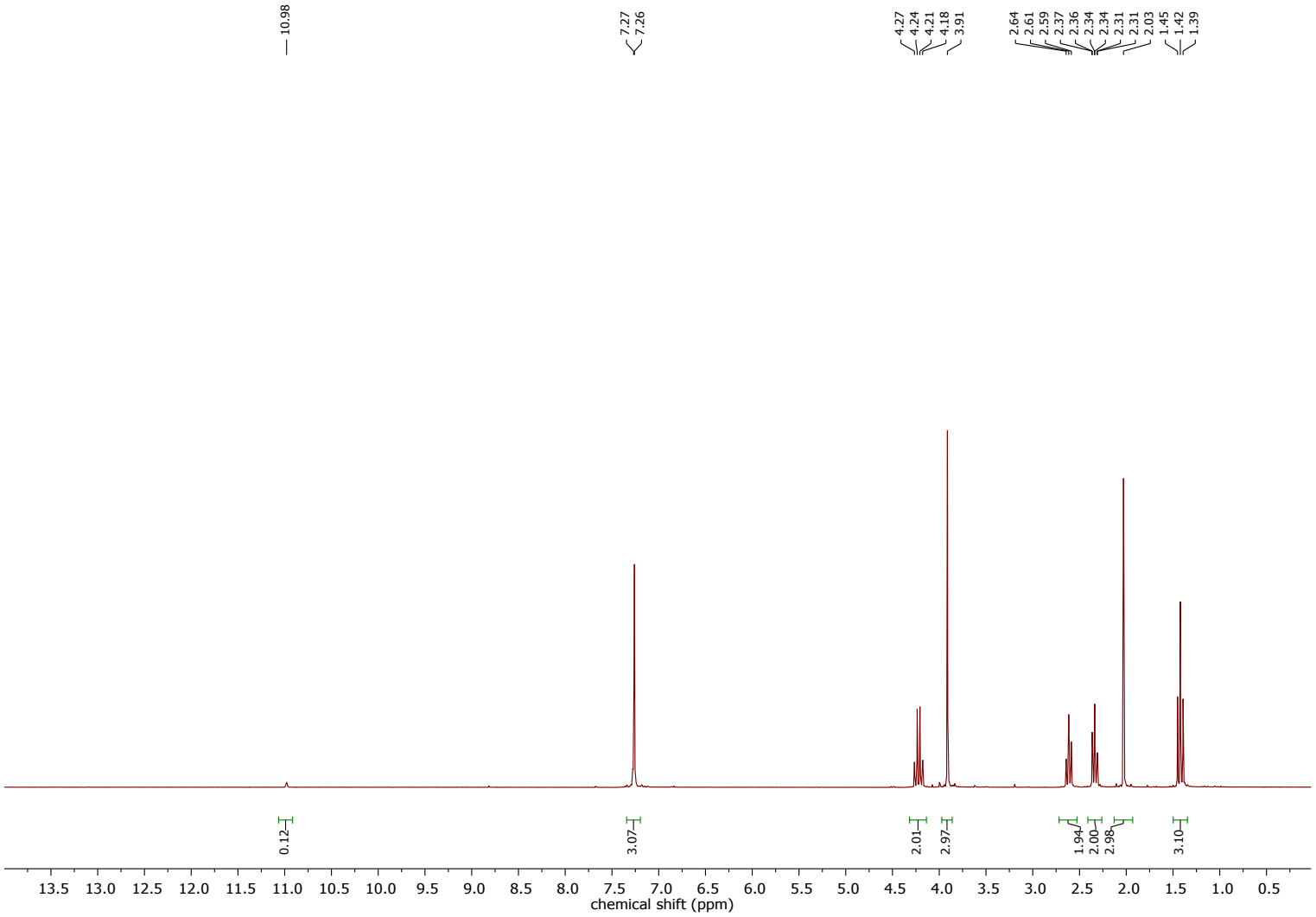

Fig S2. ^{13}C NMR of **EMIMLev** at 25 °C

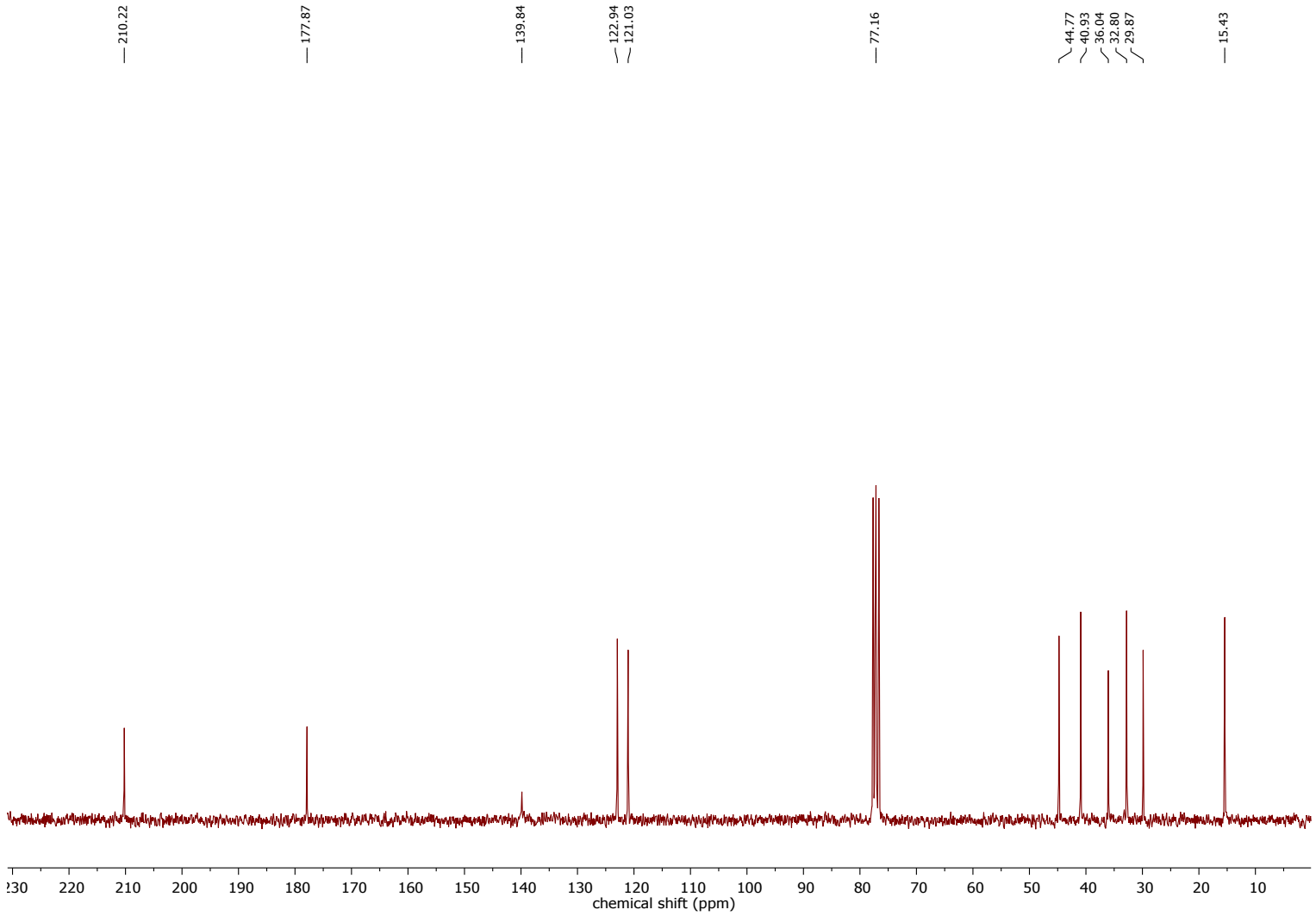

Fig S3. ^{1}H NMR of **EMIMLev** (25 °C) recycled after the second cycle of dissolution of MCC at 100 °C

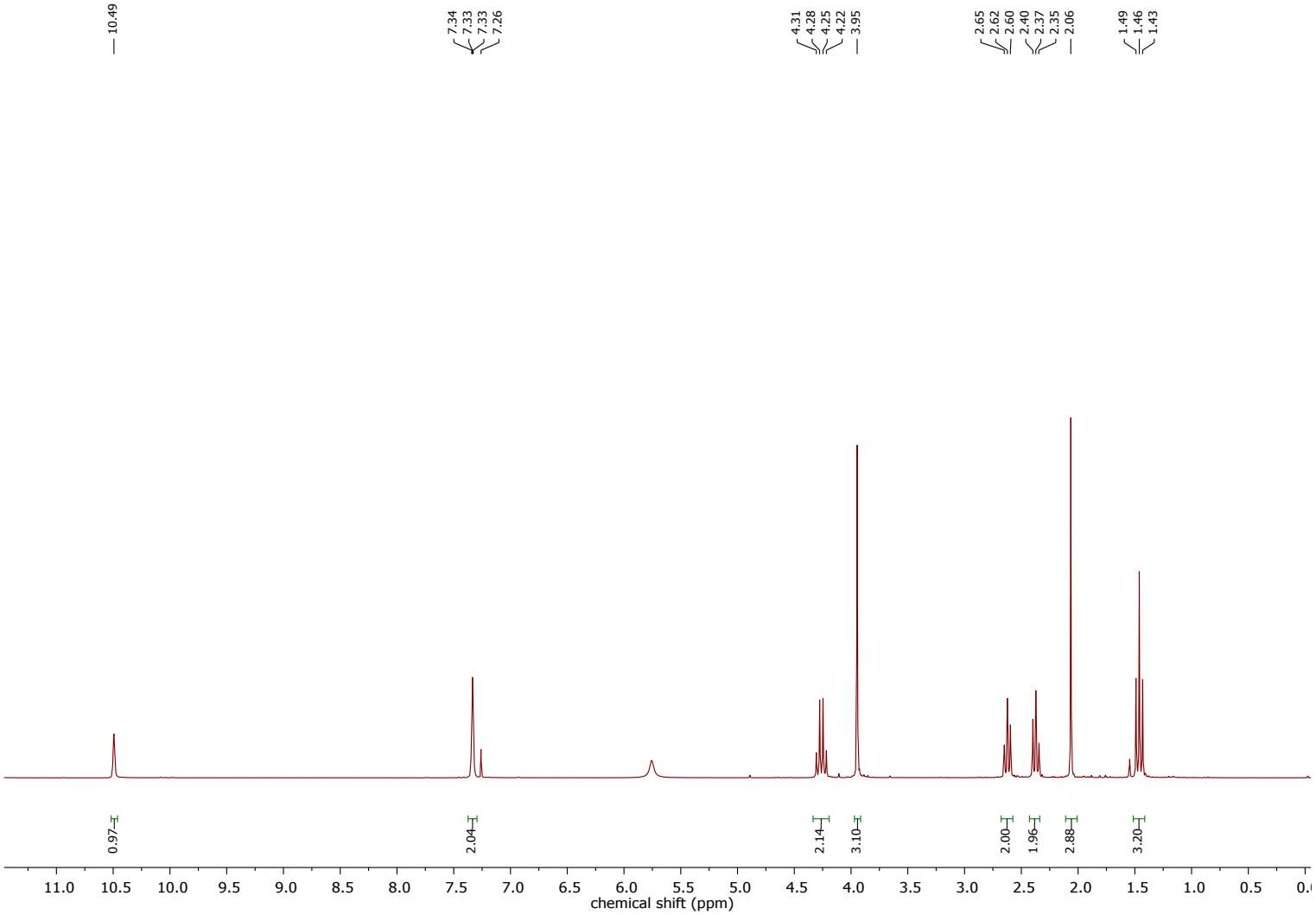

Fig S4. ^{1}H NMR of **EMIMLev** (coaxial, 25 °C) after 12h at 120 °C (thermal stability test)

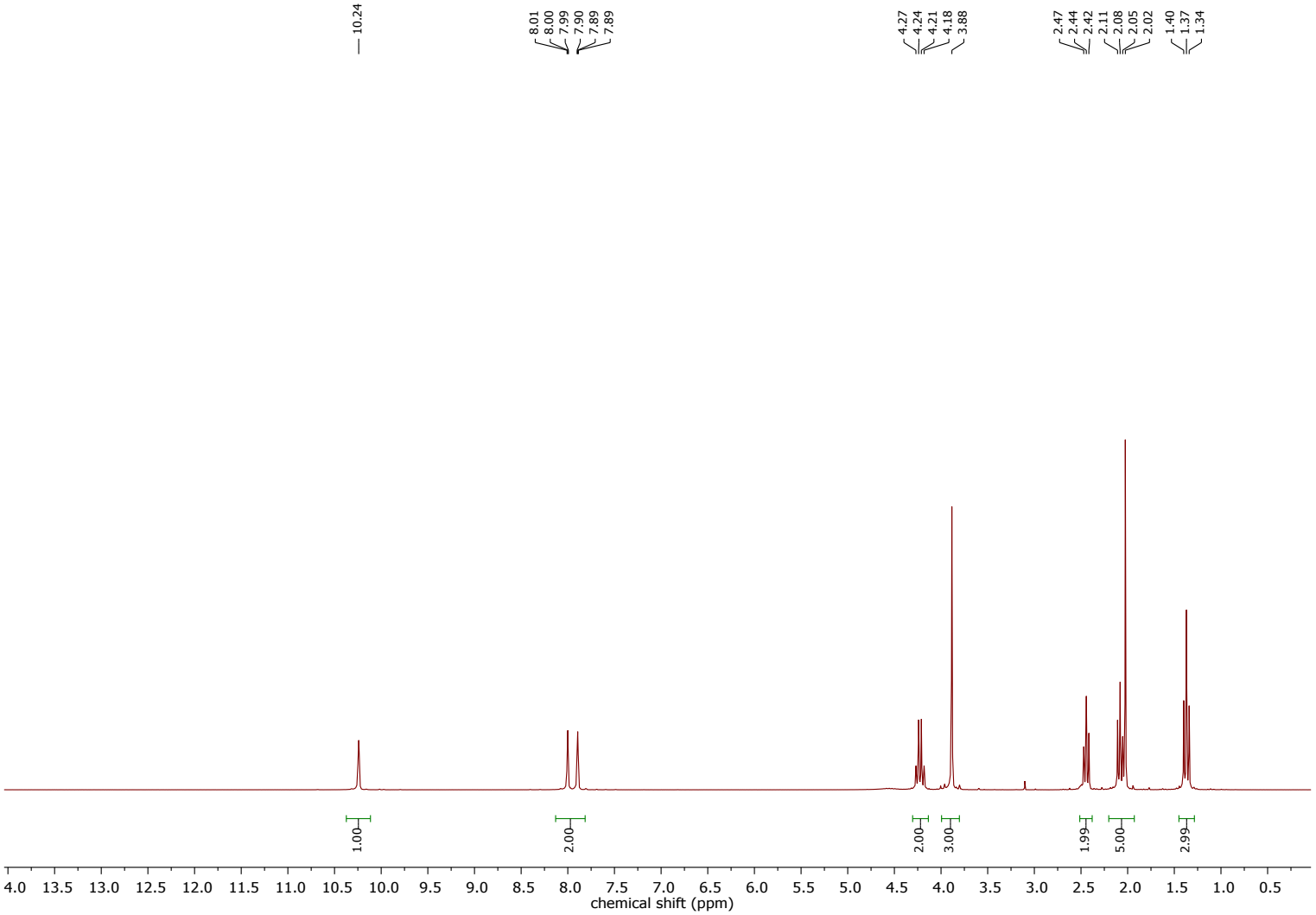

Fig S5. ^{1}H NMR of **BMIMLev** at 25 °C

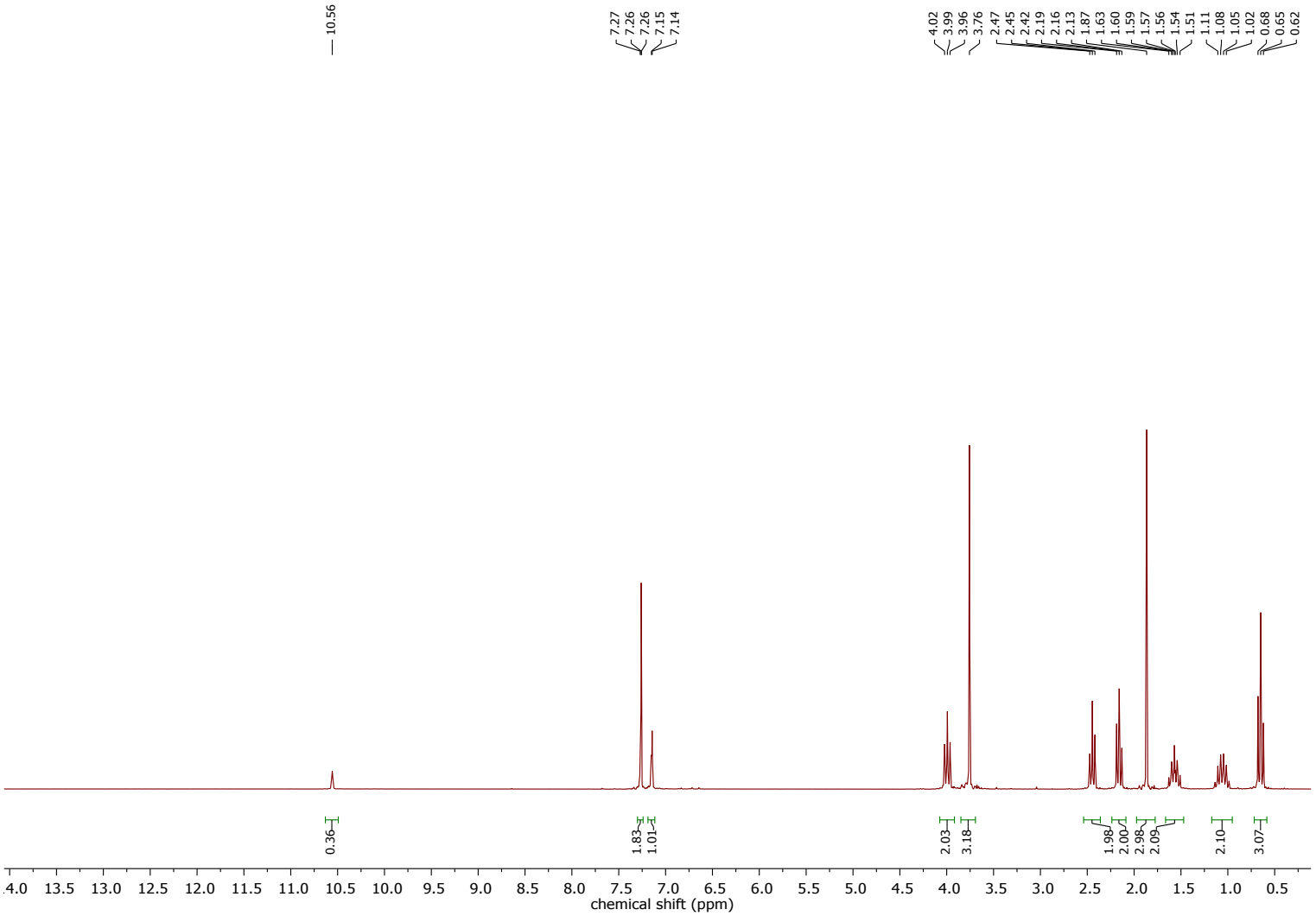

Fig S6. ^{13}C NMR of **BMIMLev** at 25 °C

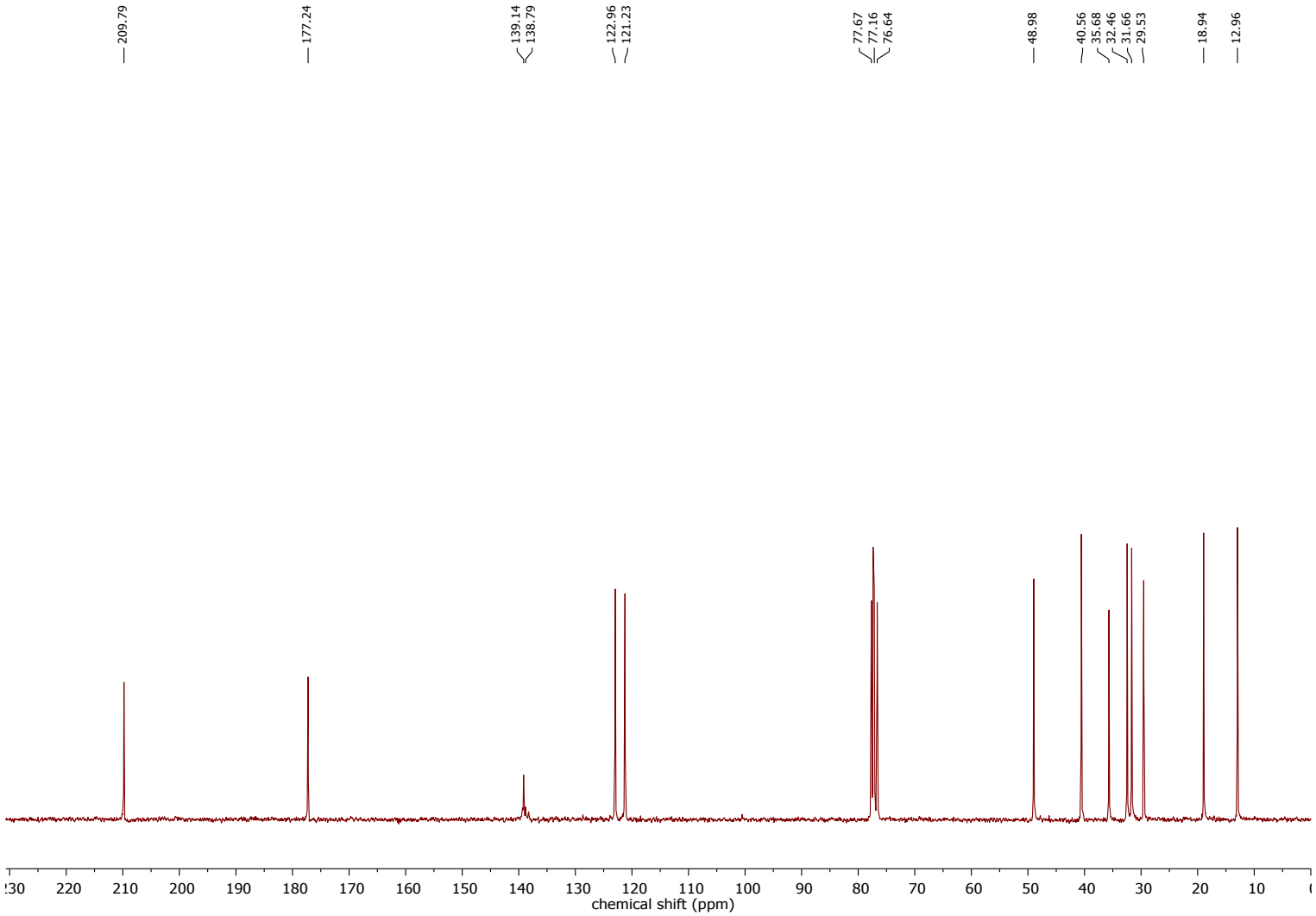

Fig S7. ^{1}H NMR of **N_{8881}Lev** at 25 °C

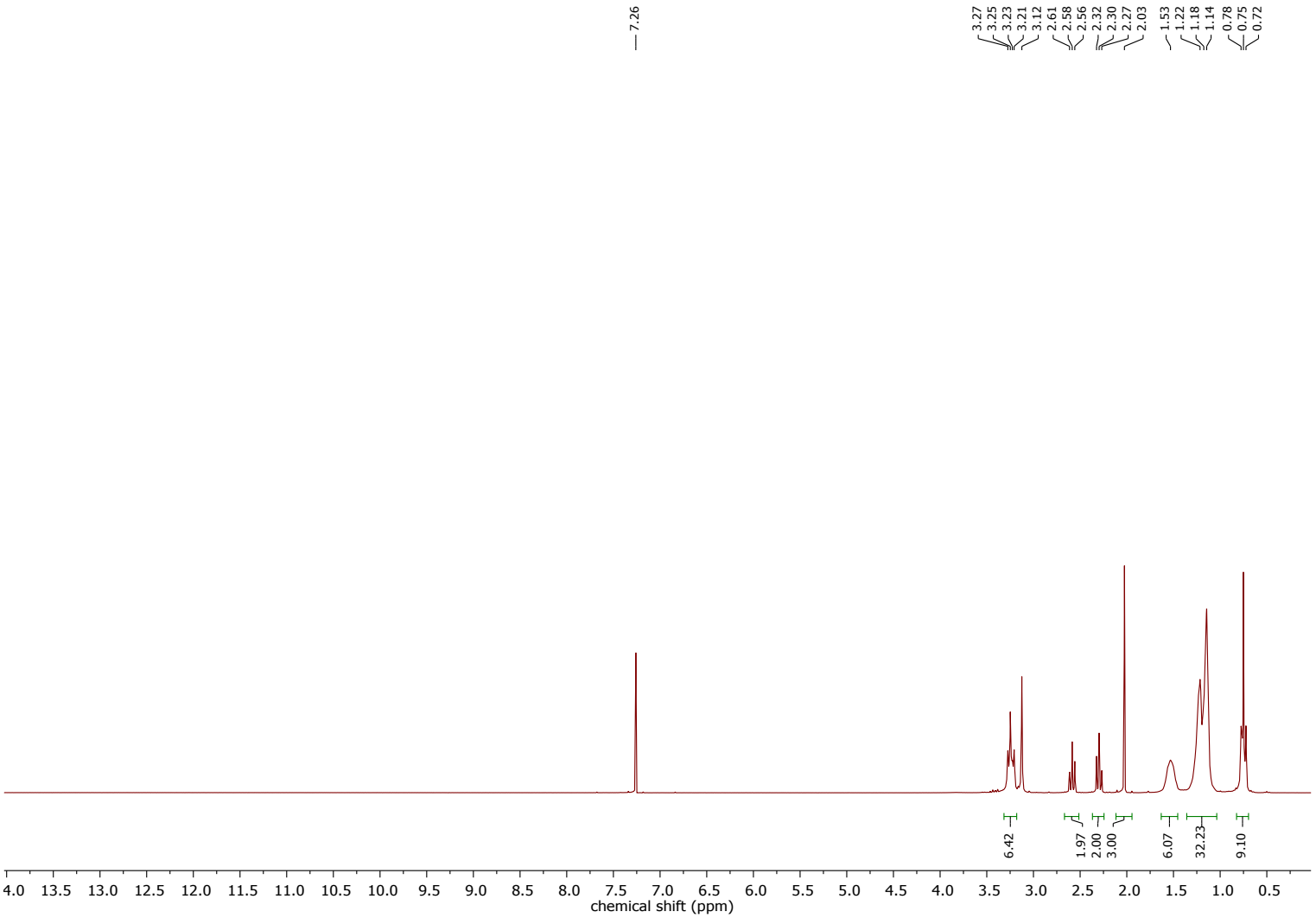

Fig S8. ^{13}C NMR of **N_{8881}Lev** at 25 °C

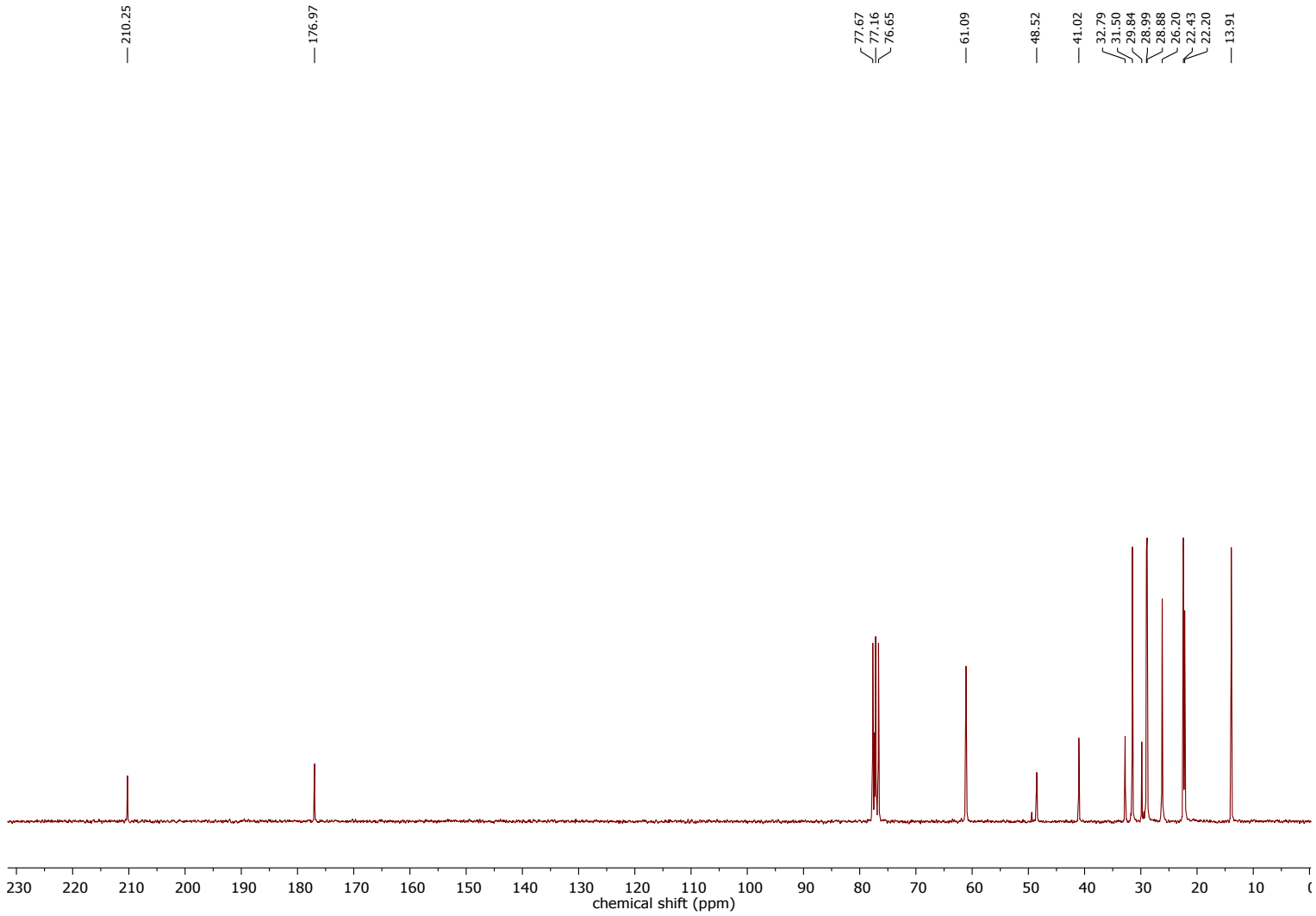

Fig S9. ^{1}H NMR of **P_{8881}Lev** at 25 °C

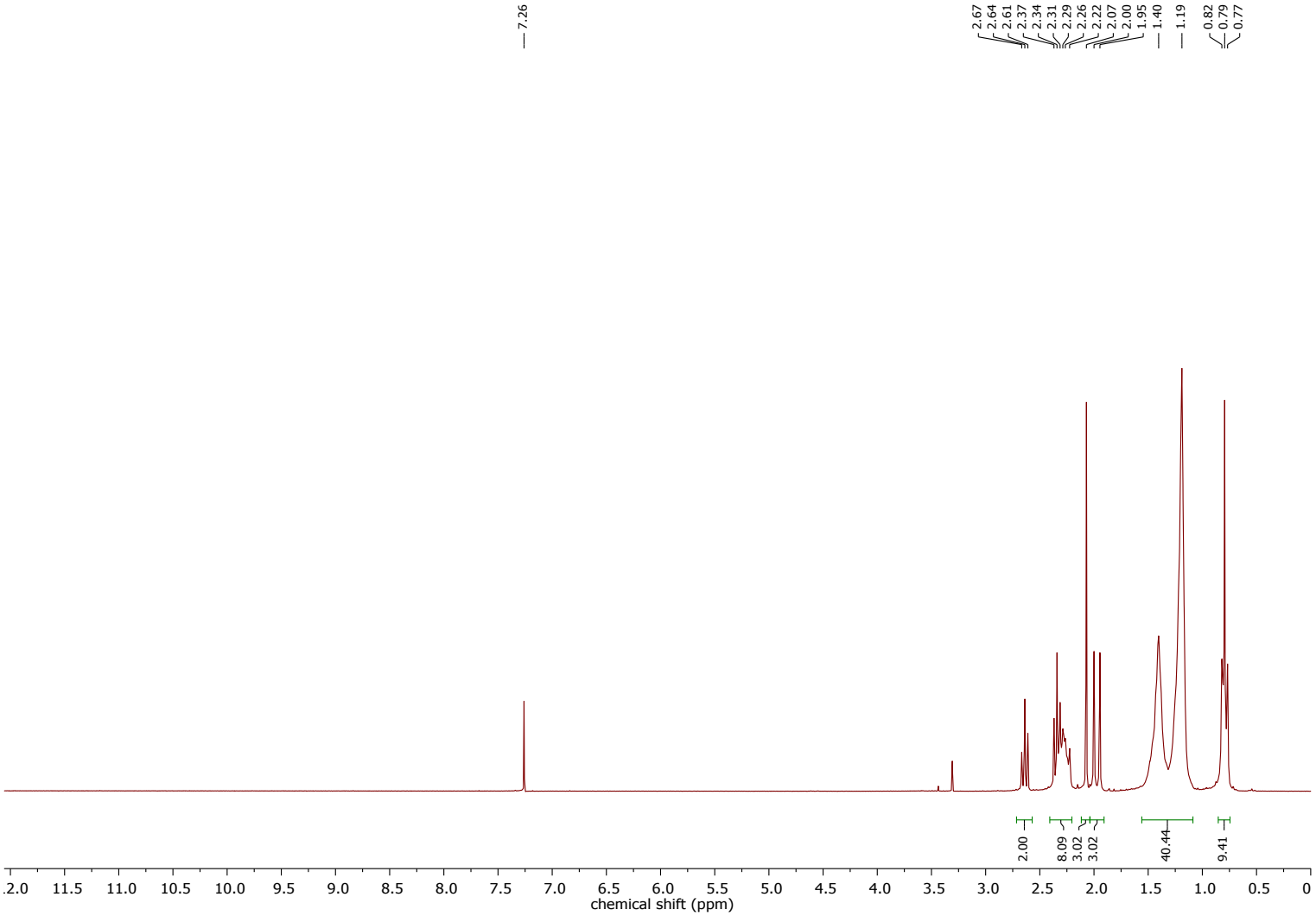

Fig S10. ^{13}C NMR of **P_{8881}Lev** at 25 °C

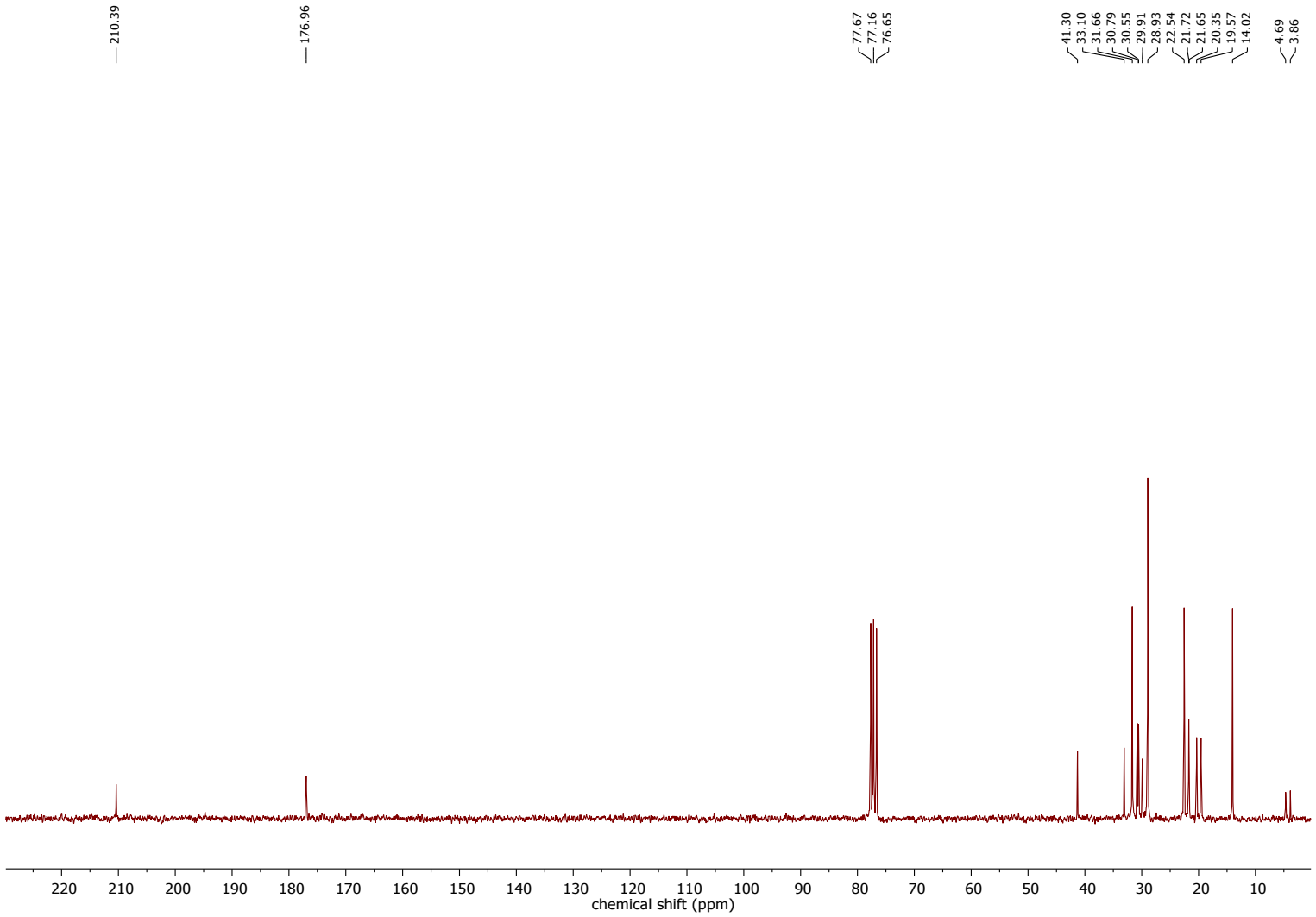

Fig S11. IR of **EMIMLev** at 25 °C

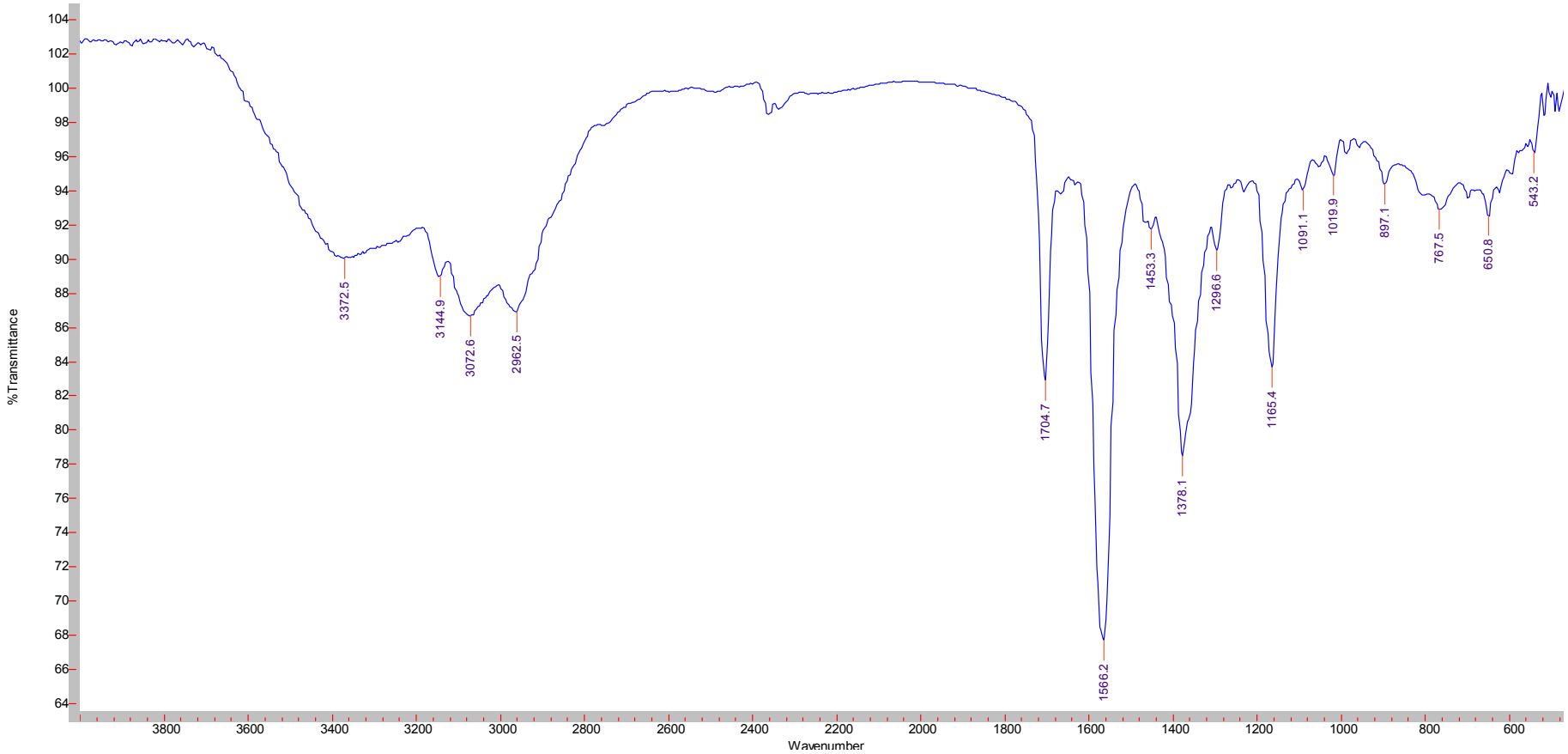

Fig S12. IR of **BMIMLev** at 25 °C

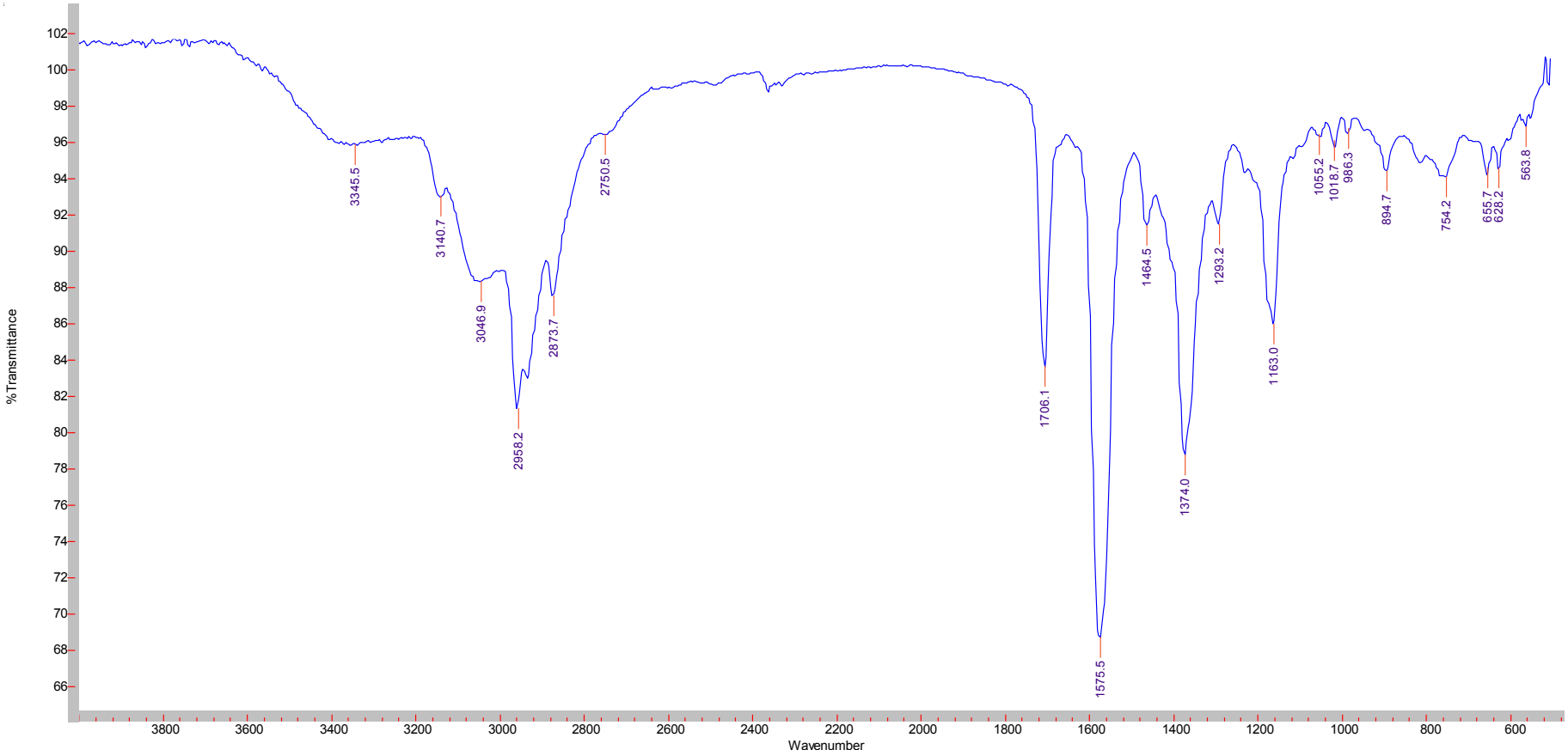

Fig S13. IR of **N_{8881}Lev** at 25 °C

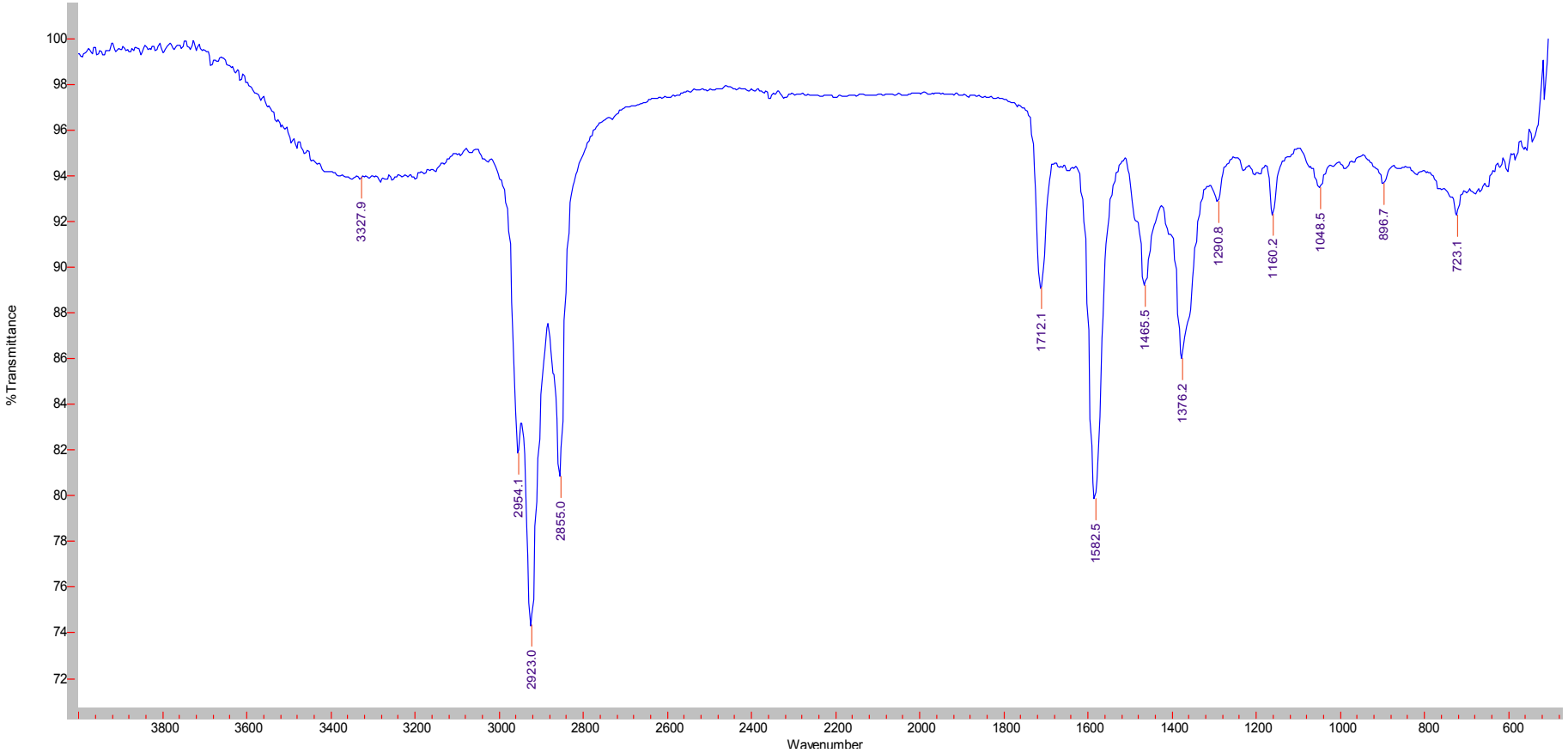

Fig S14. IR of **P_{8881}Lev** at 25 °C

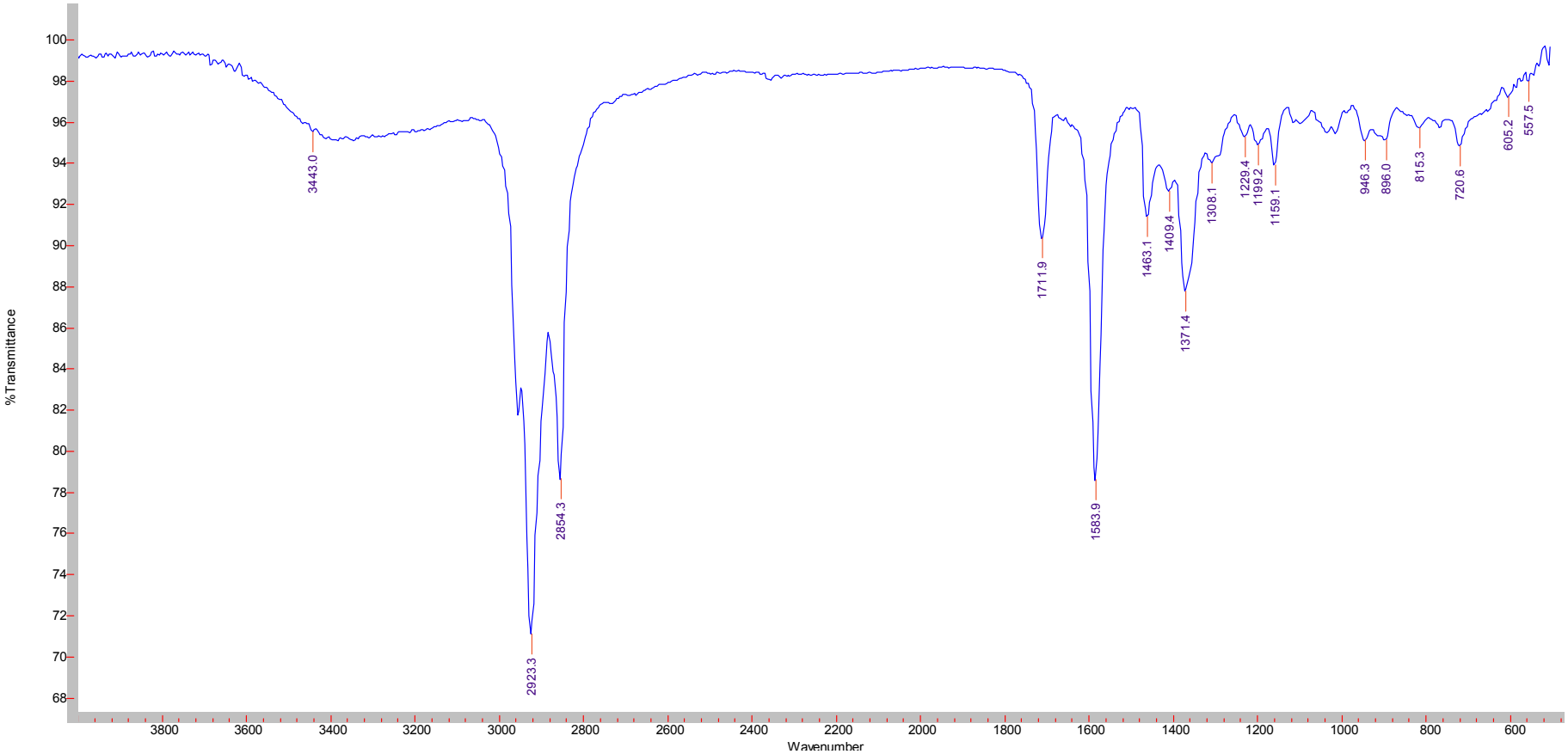

Fig S15. Thermal gravimetric analysis (TGA) of **EMIMLev**

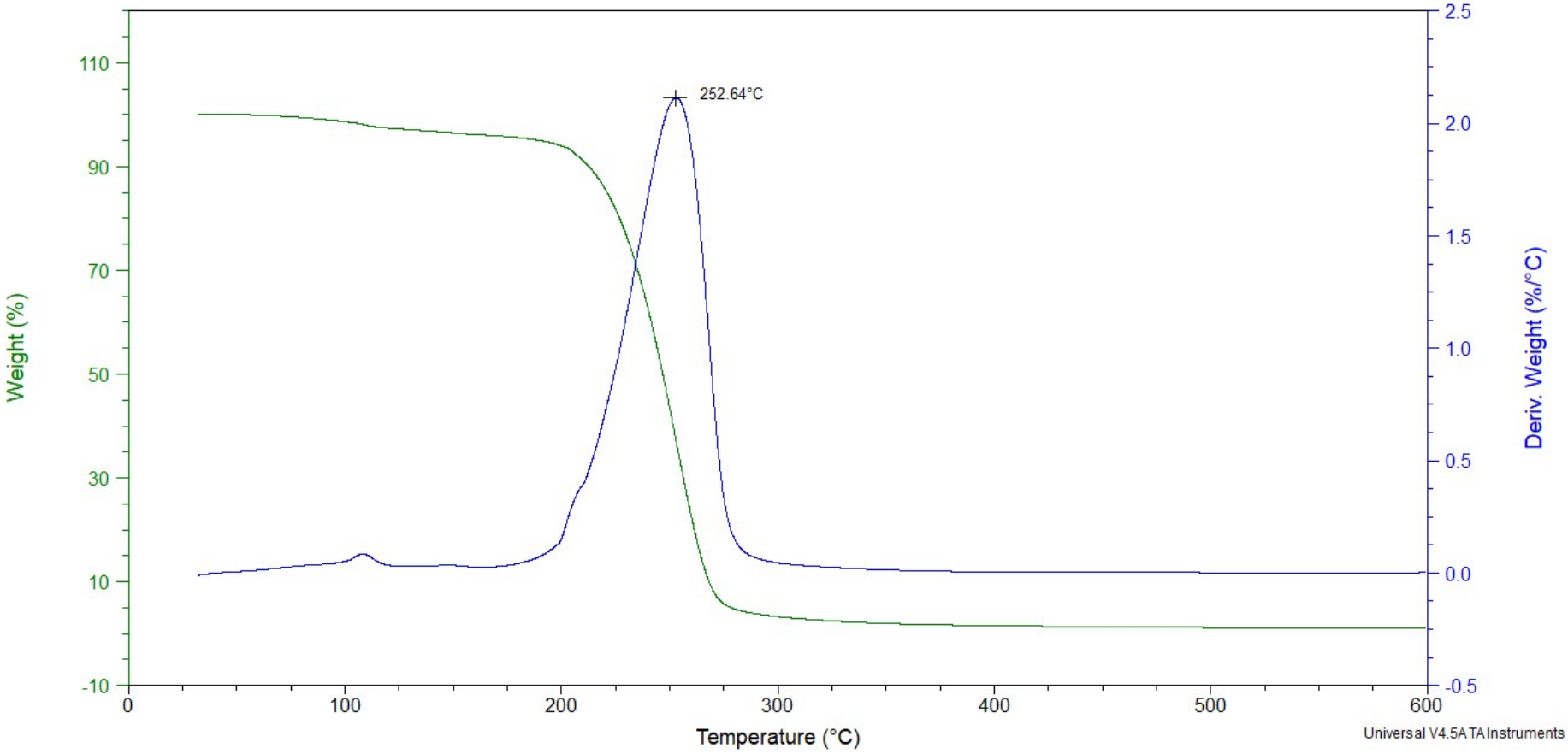

Fig S16. Thermal gravimetric analysis (TGA) of **BMIMLev**

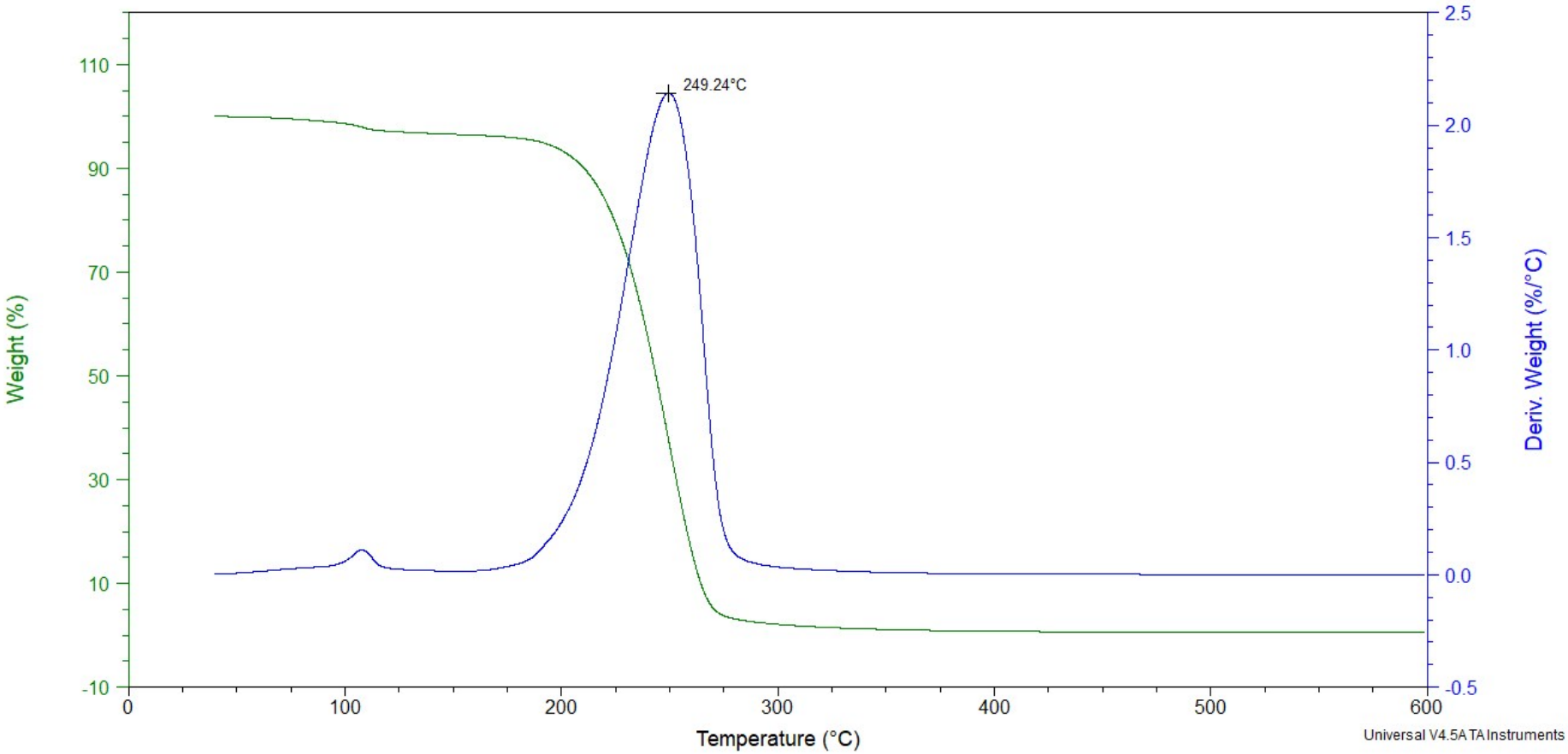

Fig S17. Thermal gravimetric analysis (TGA) of **N_{8881}Lev**

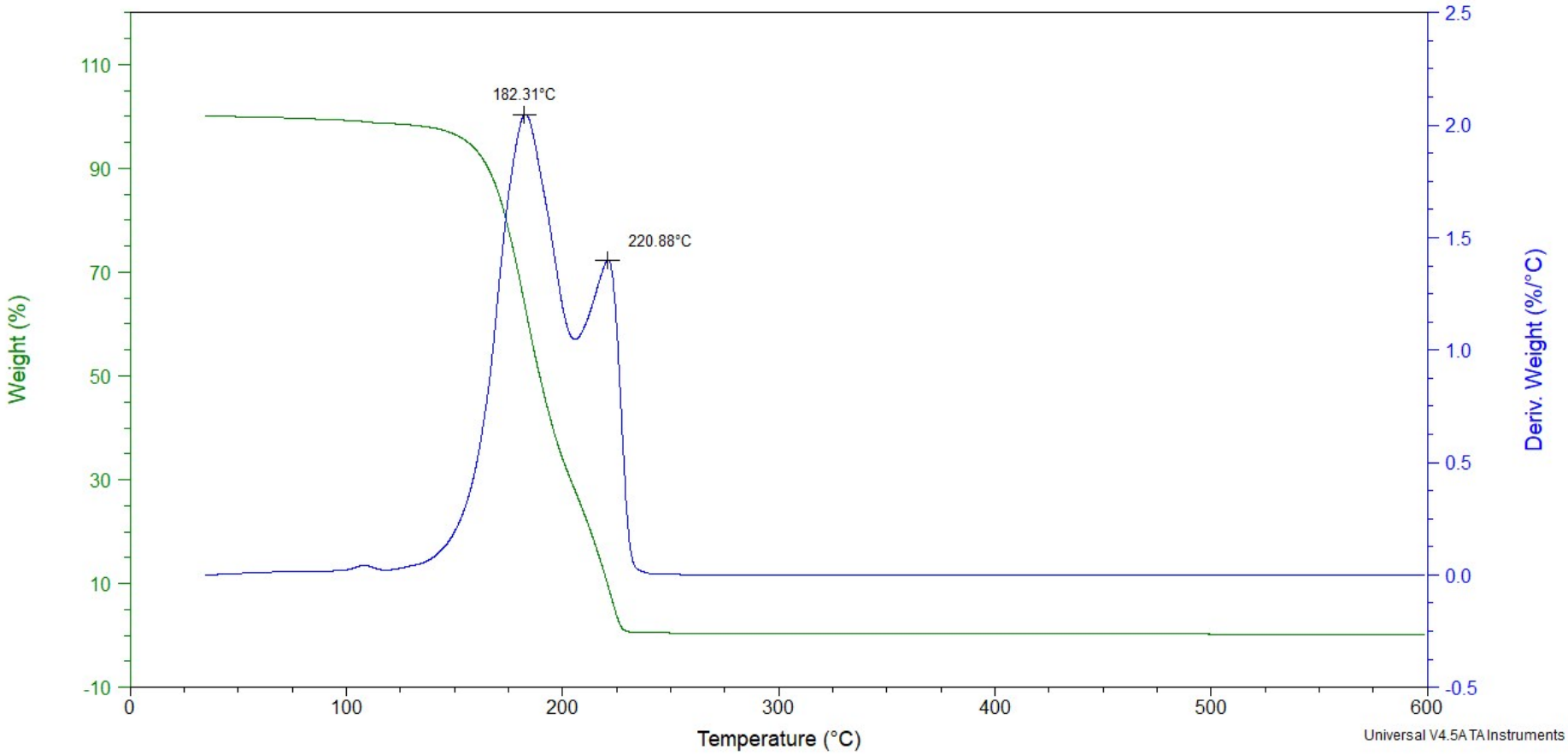

Fig S18. Thermal gravimetric analysis (TGA) of **P_{8881}Lev**

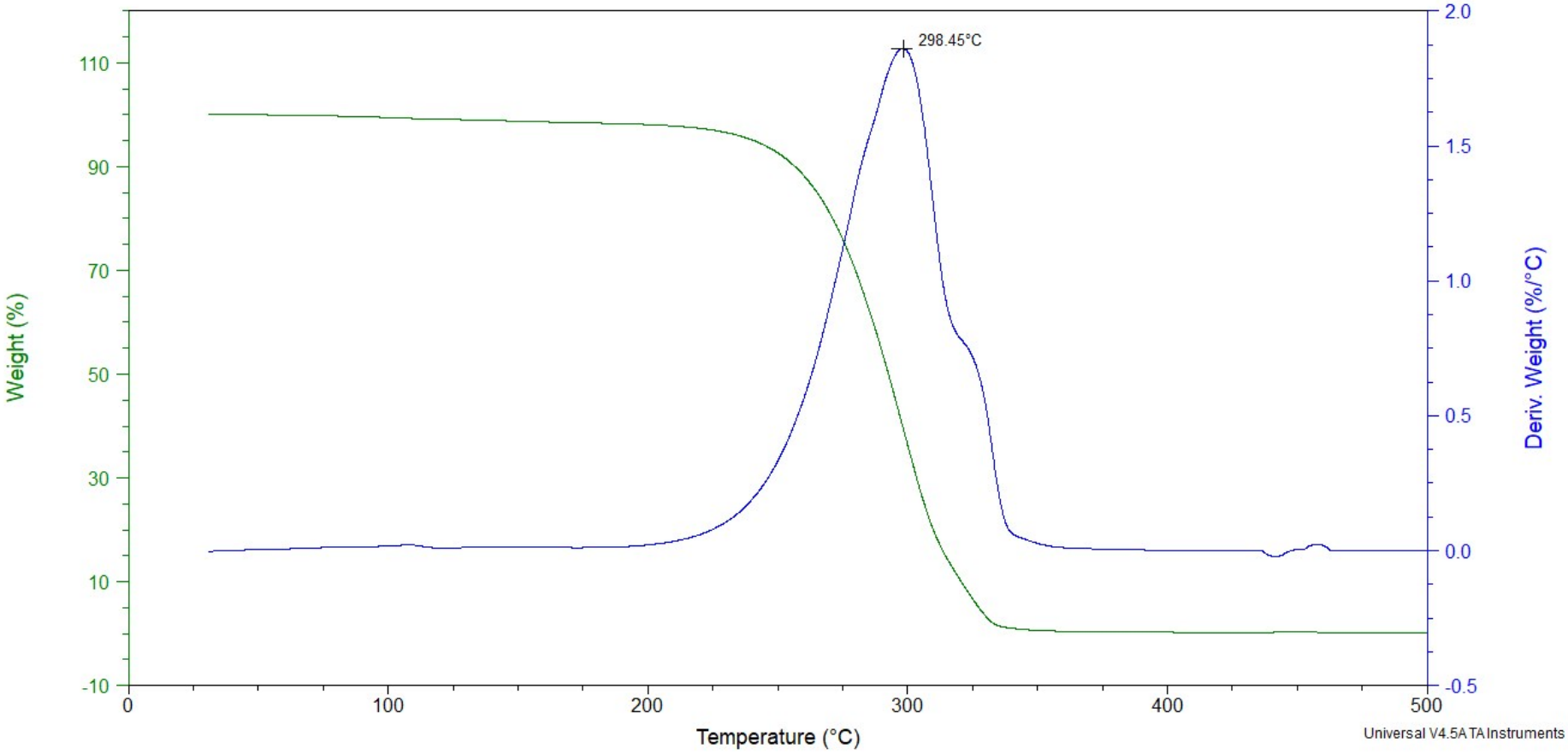

Fig S19: Pictures of dissolved MCC in **EMIMLev**: 25 °C, 6 wt% (**A**); 40 °C, 8 wt% (**B**); 60 °C, 18 wt%(**C**); 80 °C, 26 wt%(**D**); 100 °C, 29 wt%(**E**)

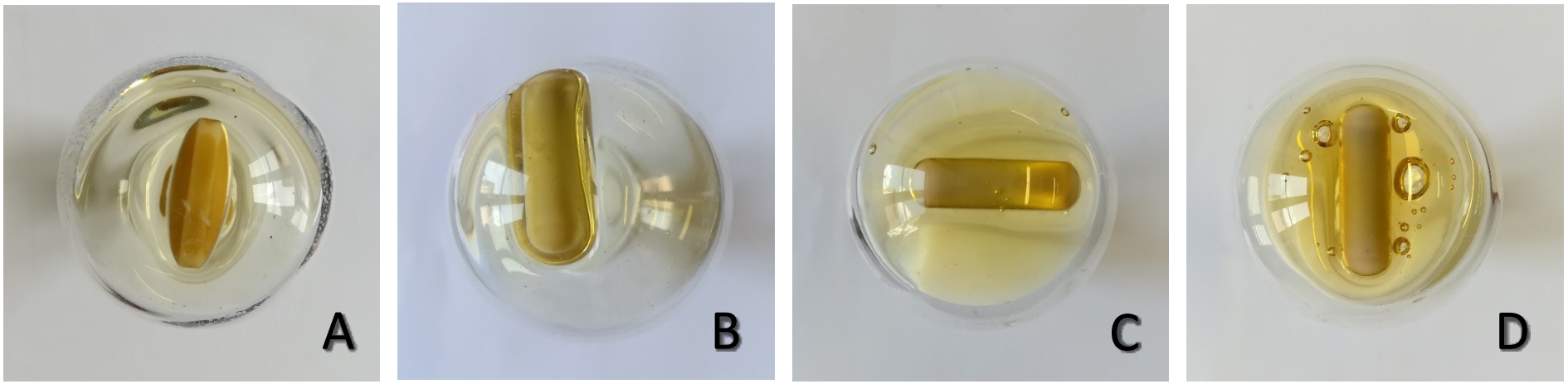

Fig S20: Picture of undissolved MCC in **EMIMLev** (100 °C, 30 wt%)

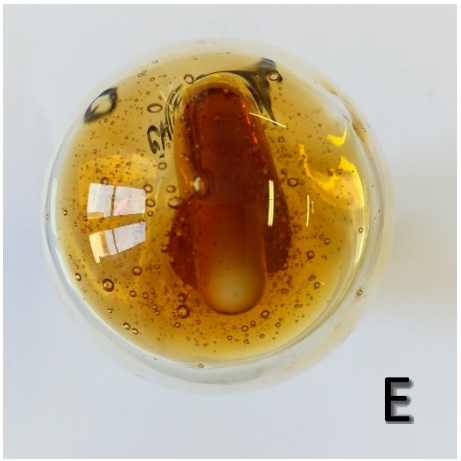

Fig S21: Dissolved MCC in **EMIMLev**, at 60 °C, with addition of a precise amount (10% mol) of contaminants: H_2O (**A**), MeOH (**B**), EtOH (**C**)

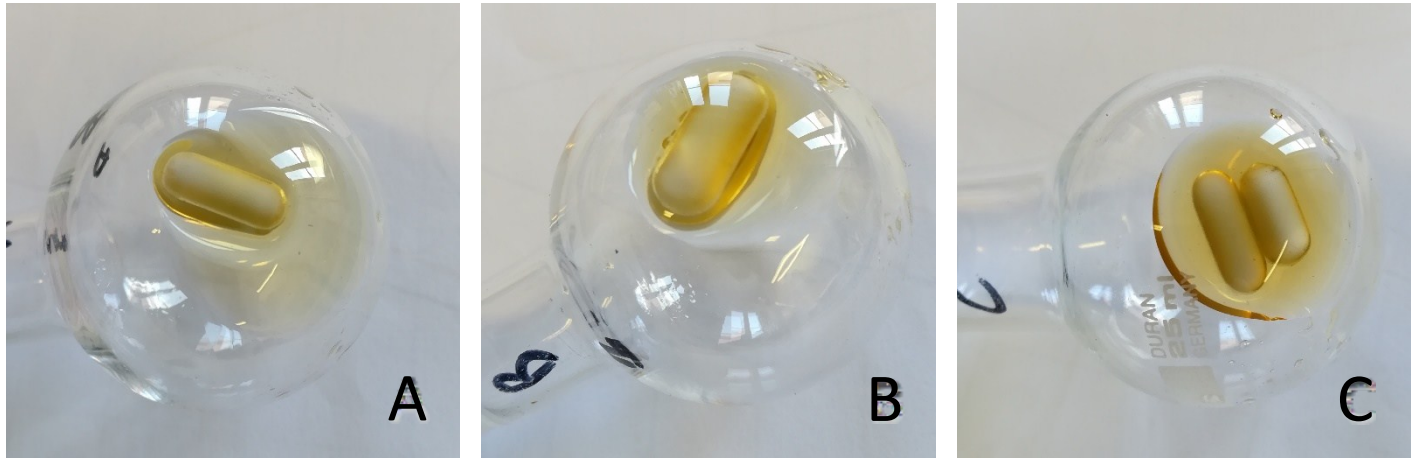

Fig S22: Pictures of under vacuum dissolved MCC in **EMIMLev**: 25 °C, 8 wt% (**A**); 40 °C, 12 wt% (**B**); 60 °C, 20 wt%(**C**); 80 °C, 33 wt%(**D**); 100 °C, 38 wt%(**E**)

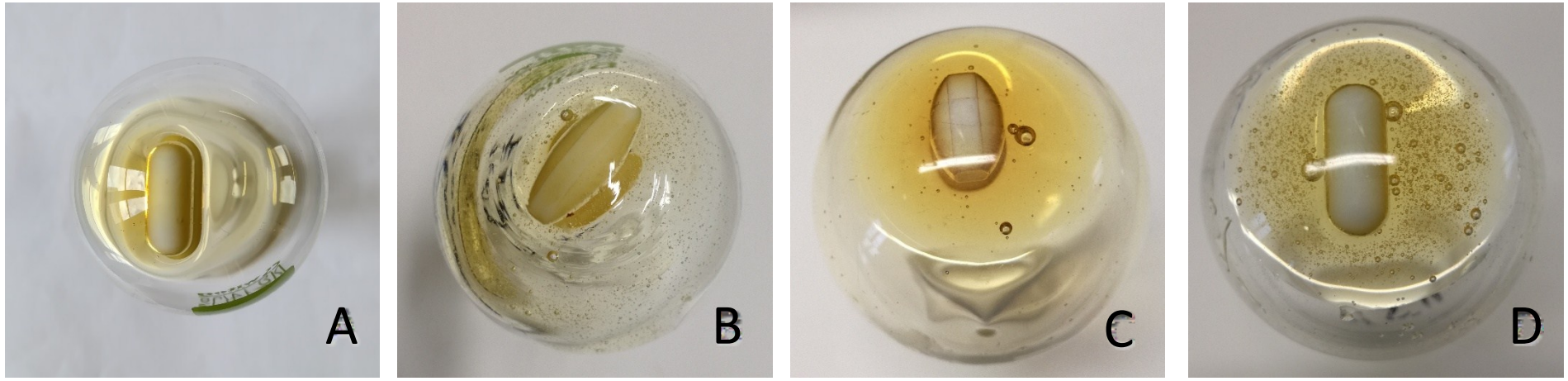

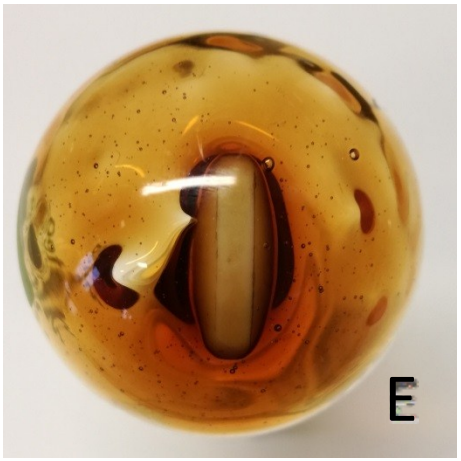

Fig S23: Pictures of under vacuum undissolved MCC in **EMIMLev** (**A**) (100 °C, 38.5 wt%) and under vacuum dissolved MCC in two-time recycled **EMIMLev** (**B**) (100 °C, 37% MCC)

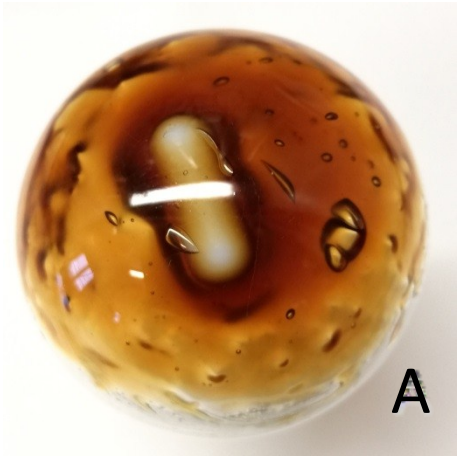

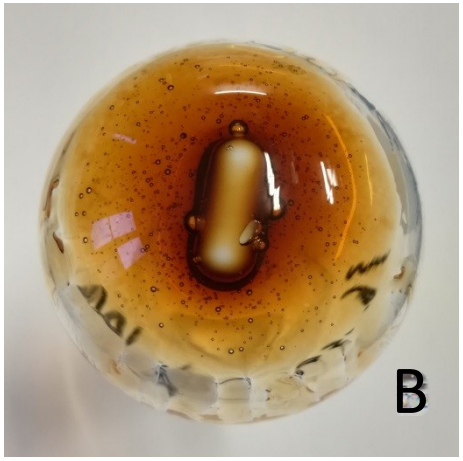

Fig S24: Picture of dissolved MCC in **BMIMLev**: 25 °C, 2 wt% (**A**); 40 °C, 7 wt% (**B**); 60 °C, 16 wt% (**C**); 80°C, 22 wt%(**D**); 100 °C, 24 wt%(**E**)

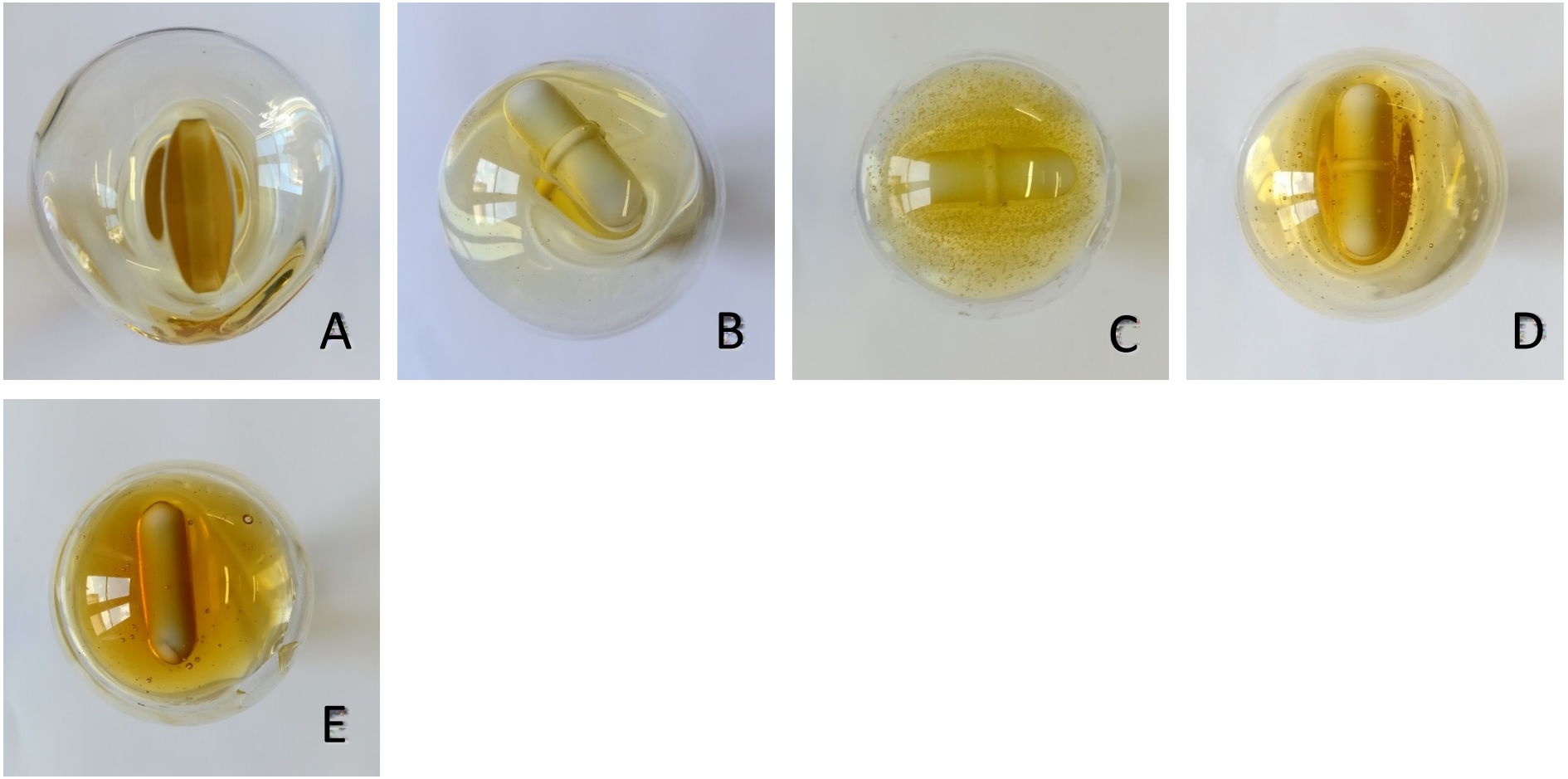

Fig S25: Picture of under vacuum dissolved MCC in **BMIMLev**: 25 °C, 3 wt%(**A**); 40 °C, 12 wt% (**B**); 60 °C, 25 wt% (**C**); 80°C, 31 wt%(**D**); 100 °C, 34 wt%(**E**)

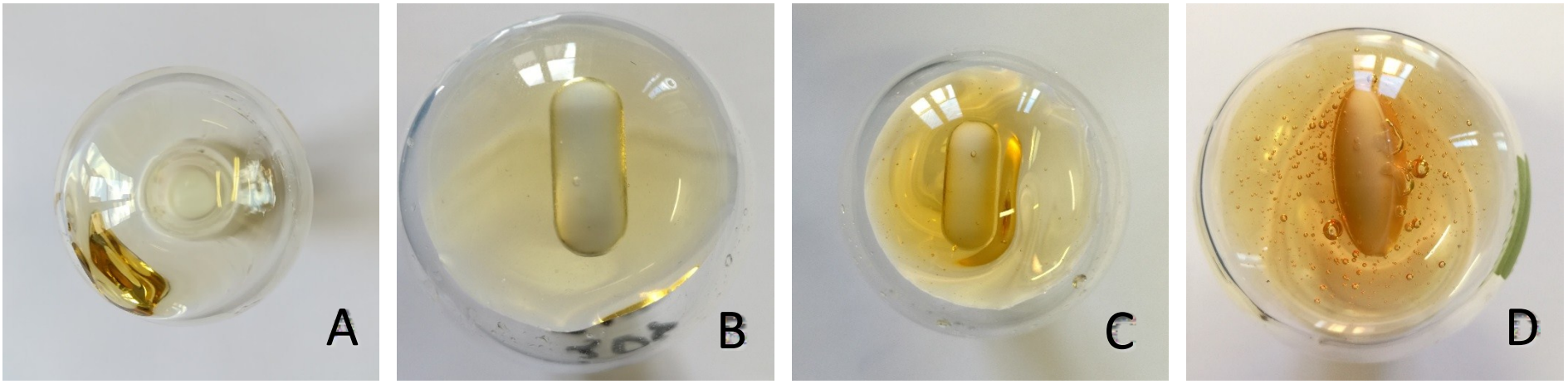

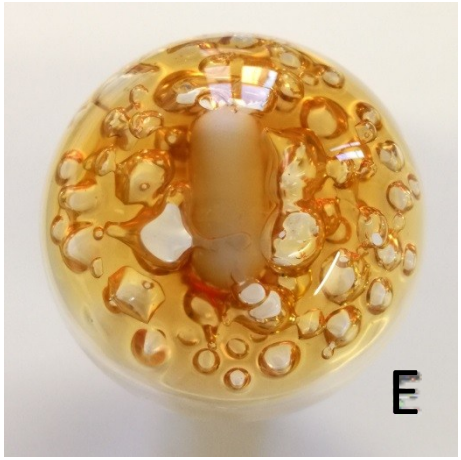

Fig S26: Picture of under vacuum undissolved MCC in **BMIMLev** (100 °C, 34.5 wt%)

Fig S27: Pictures of dissolved MCC in **N_{8881}Lev/DMSO**: 60 °C, 9 wt% (**A**); 80 °C, 10 wt% (**B**); 100 °C, 12 wt%(**C**). MCC dissolved in **N_{8881}Lev/DMSO** under vacuum at room temperature: 25 °C, 13 wt% (**D**)

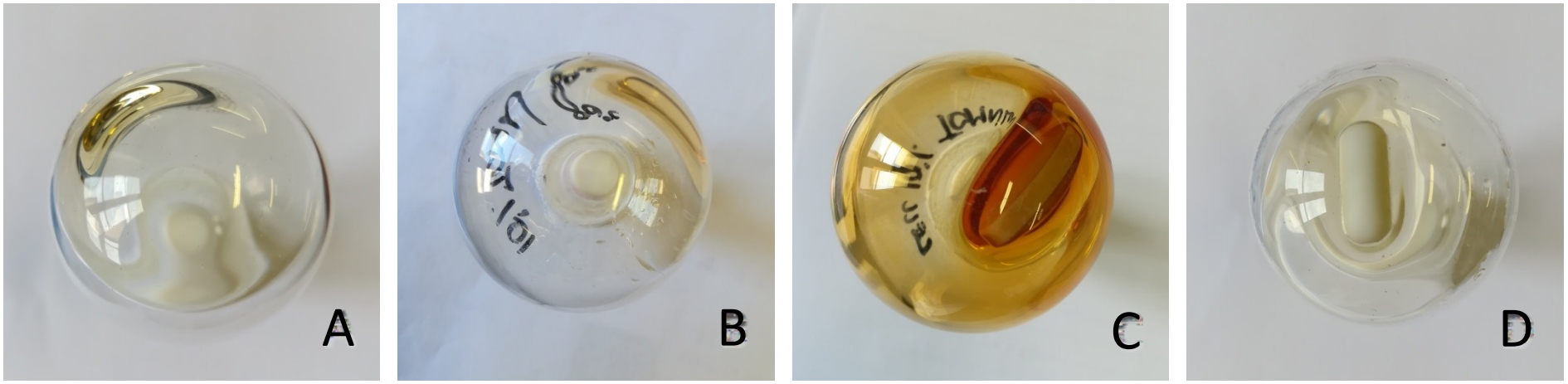

Fig S28: Pictures of dissolved MCC in **P_{8881}Lev/DMSO**: 60 °C, 7 wt% (**A**); 80 °C, 8 wt% (**B**); 100 °C, 10 wt%(**C**). Cellulose dissolved in **P_{8881}Lev/DMSO** under vacuum at room temperature: 25 °C, 11 wt% (**D**)

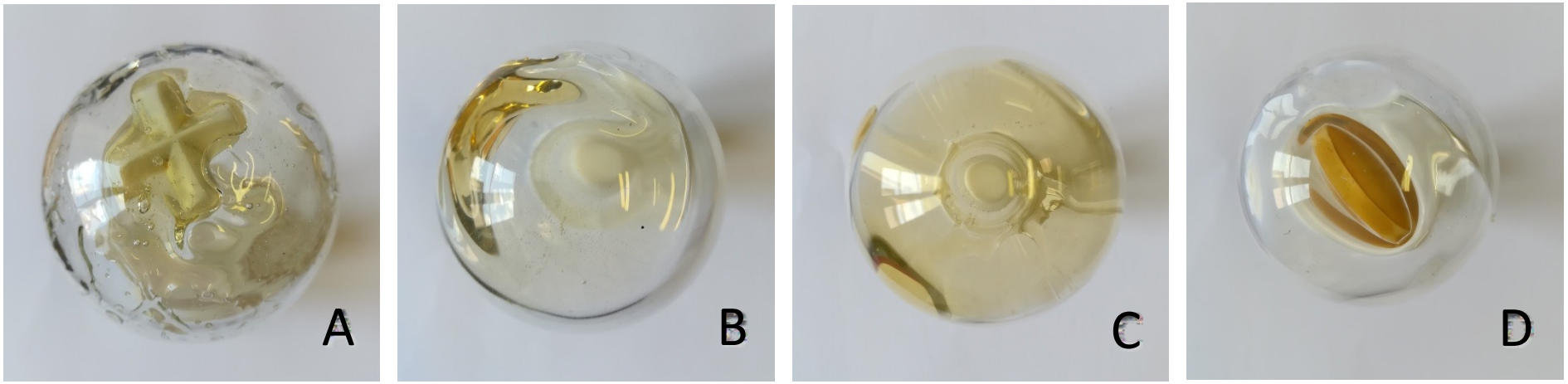

Fig S29: Optical microscopy of MCC dissolved in **EMIMLev** (100 °C, 29 wt%), 4x(**A**) and 15x (**B**)

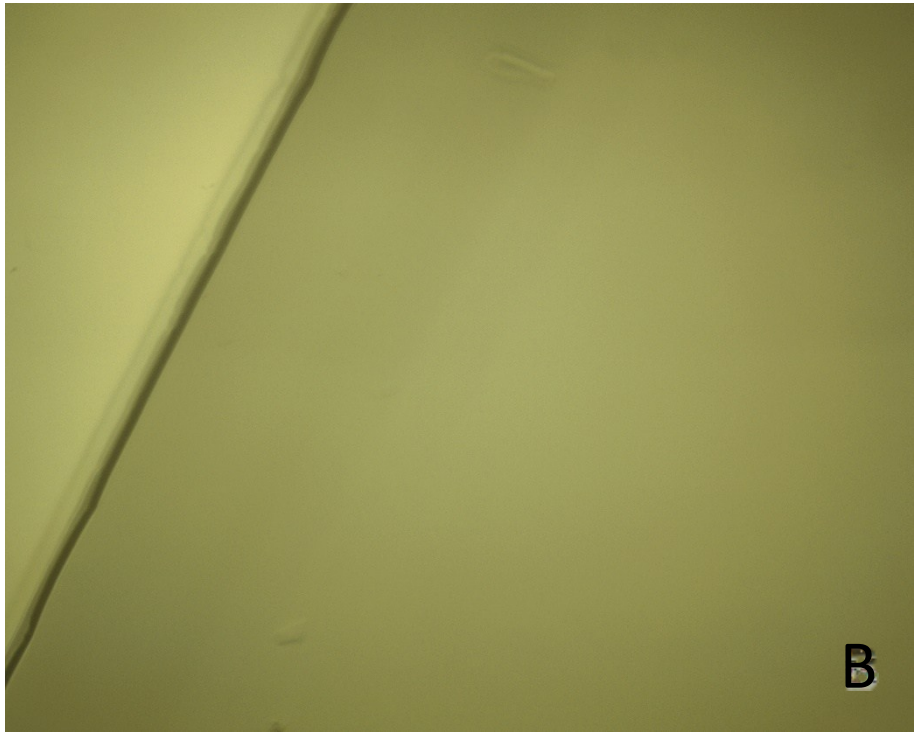

Fig S30: Microcrystalline cellulose not completely dissolved in **EMIMLev** (100 °C, 30 wt%), 4x(**A**) and 15x (**B**),

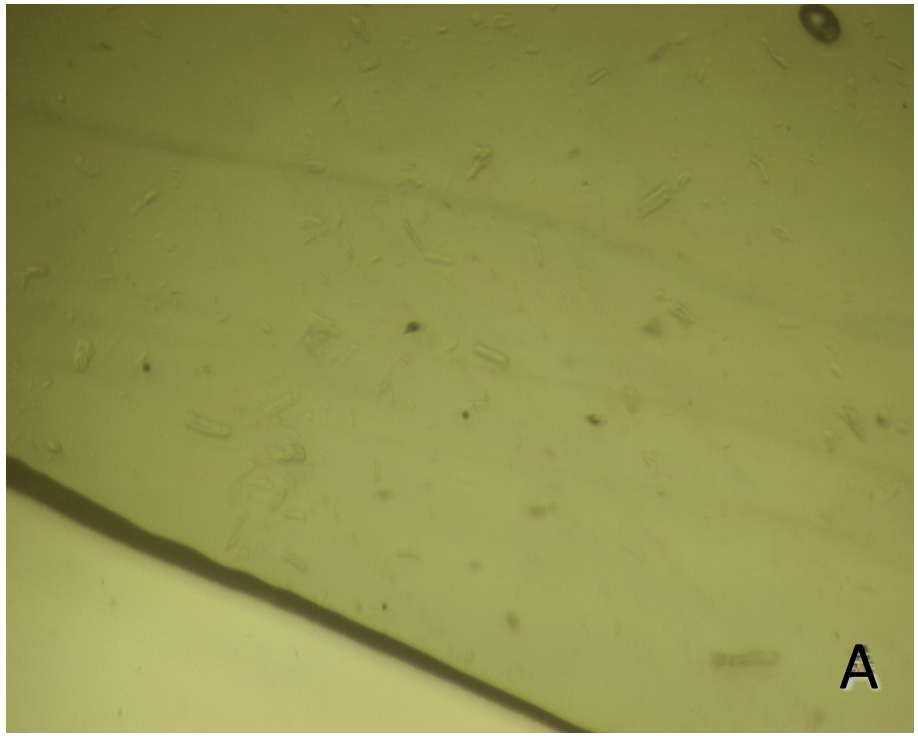

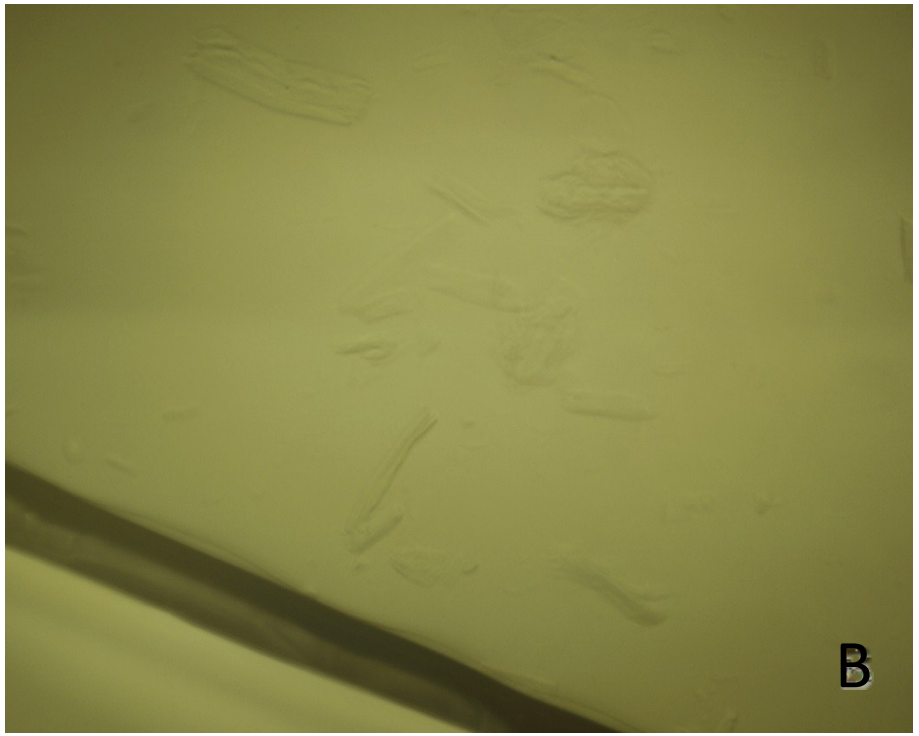

Fig S31: Optical microscopy of under vacuum dissolved MCC in **EMIMLev** (100 °C, 38 wt%), 4x(**A**) and 15x (**B**)

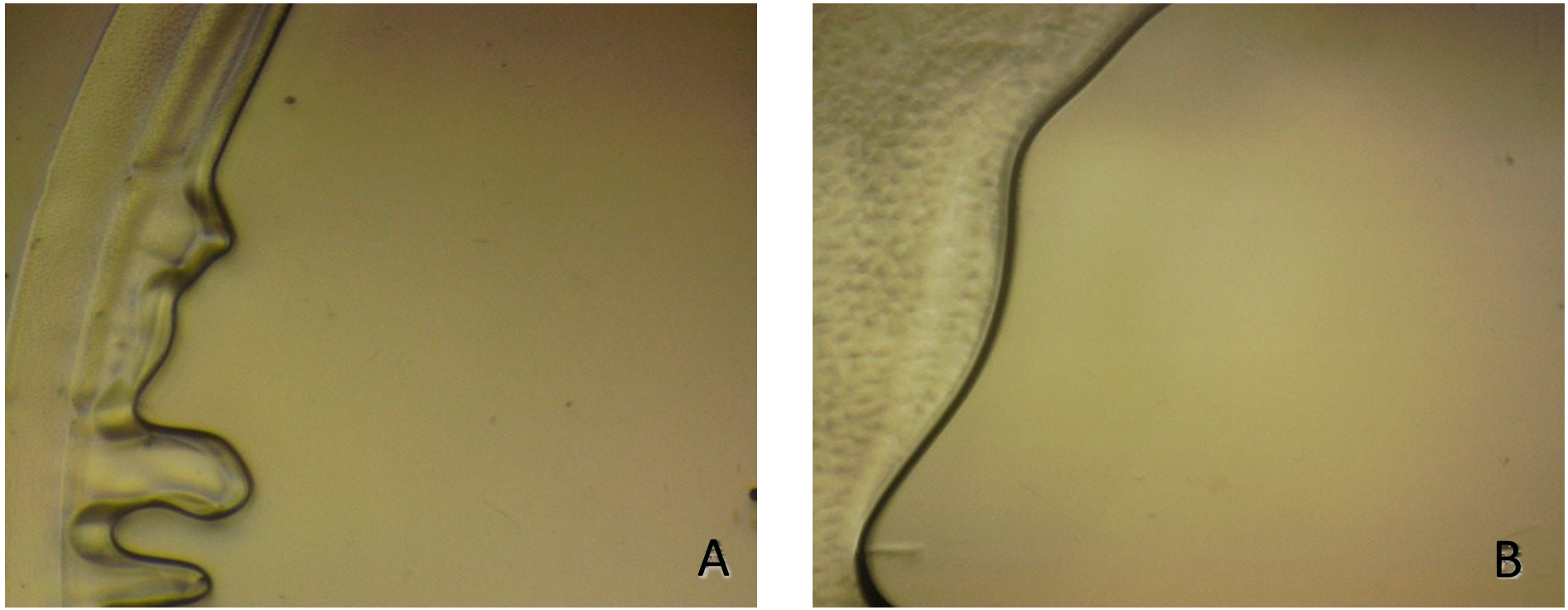

Fig S32: Optical microscopy of MCC dissolved in **BMIMLev** (100 °C, 24 wt%), 4x(**A**) and 15x (**B**)

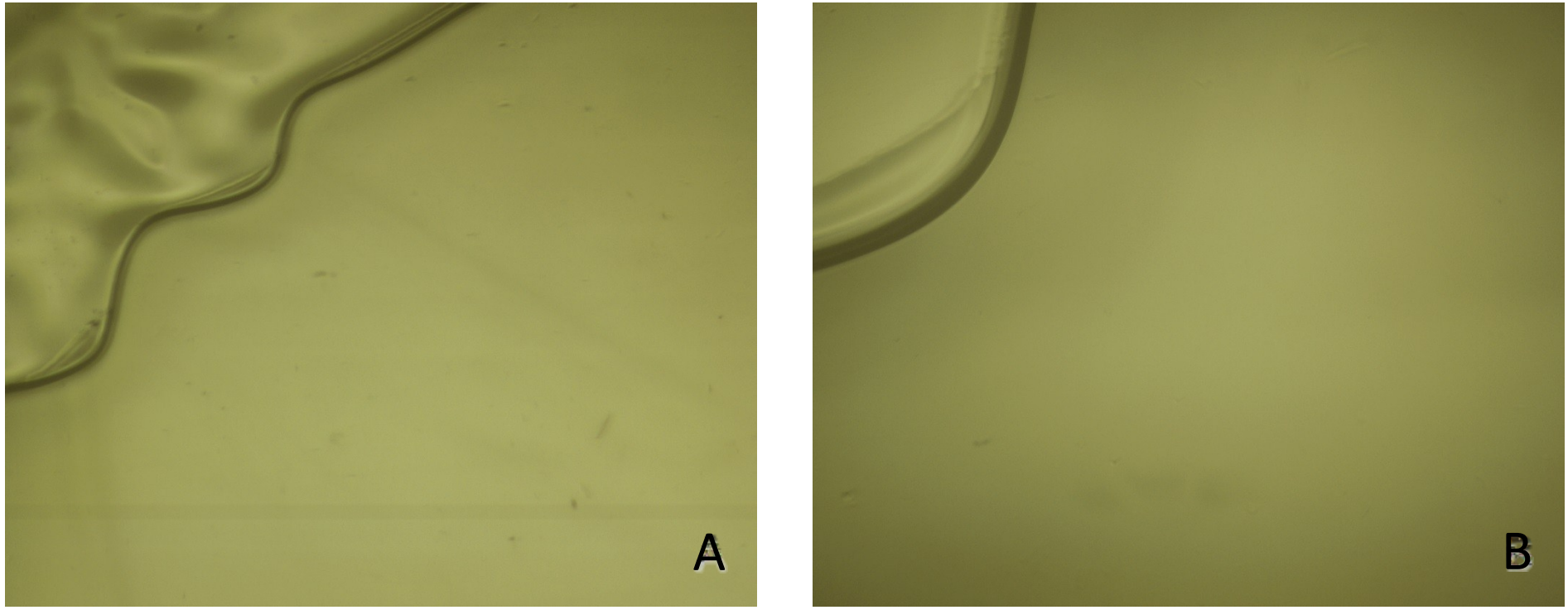

Fig S33: Optical microscopy of under vacuum dissolved MCC in **BMIMLev** (100 °C, 34 wt%), 4x(**A**) and 15x (**B**)

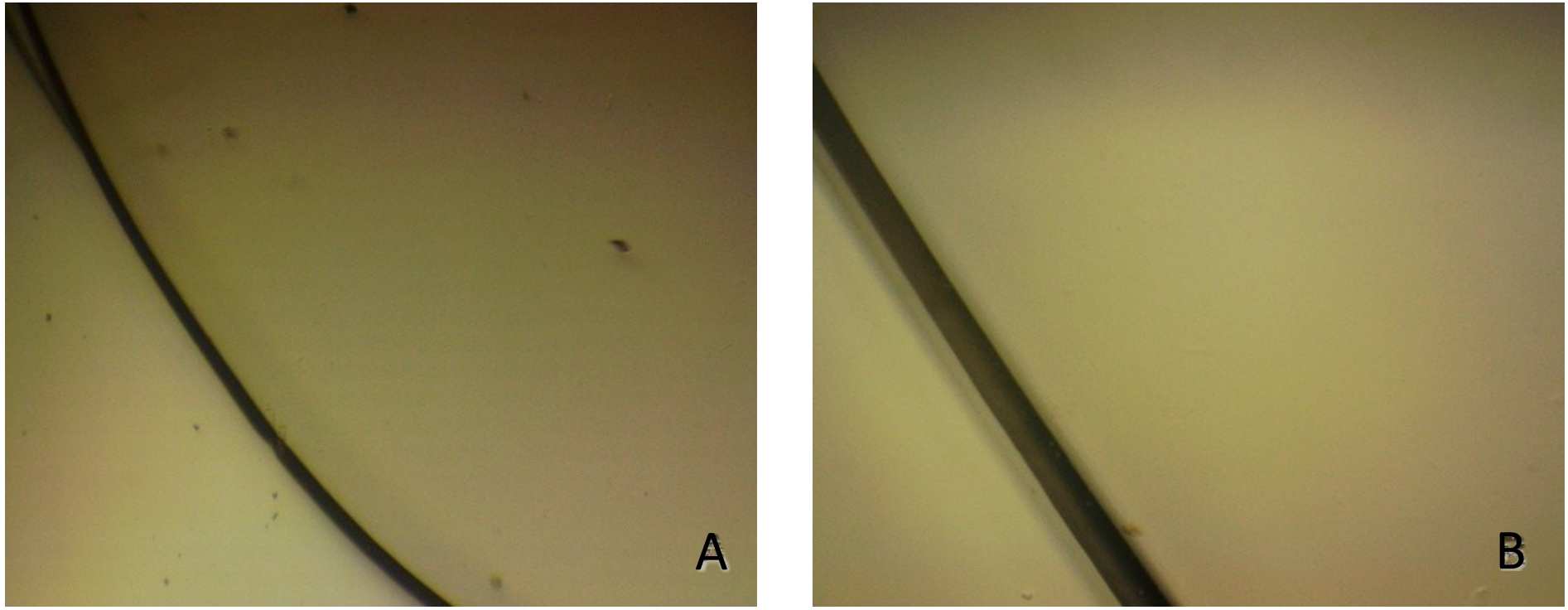

Fig S34: Optical microscopy of MCC dissolved in **N_{8881}Lev/DMSO** (100 °C, 12 wt%), 4x(**A**) and 15x (**B**)

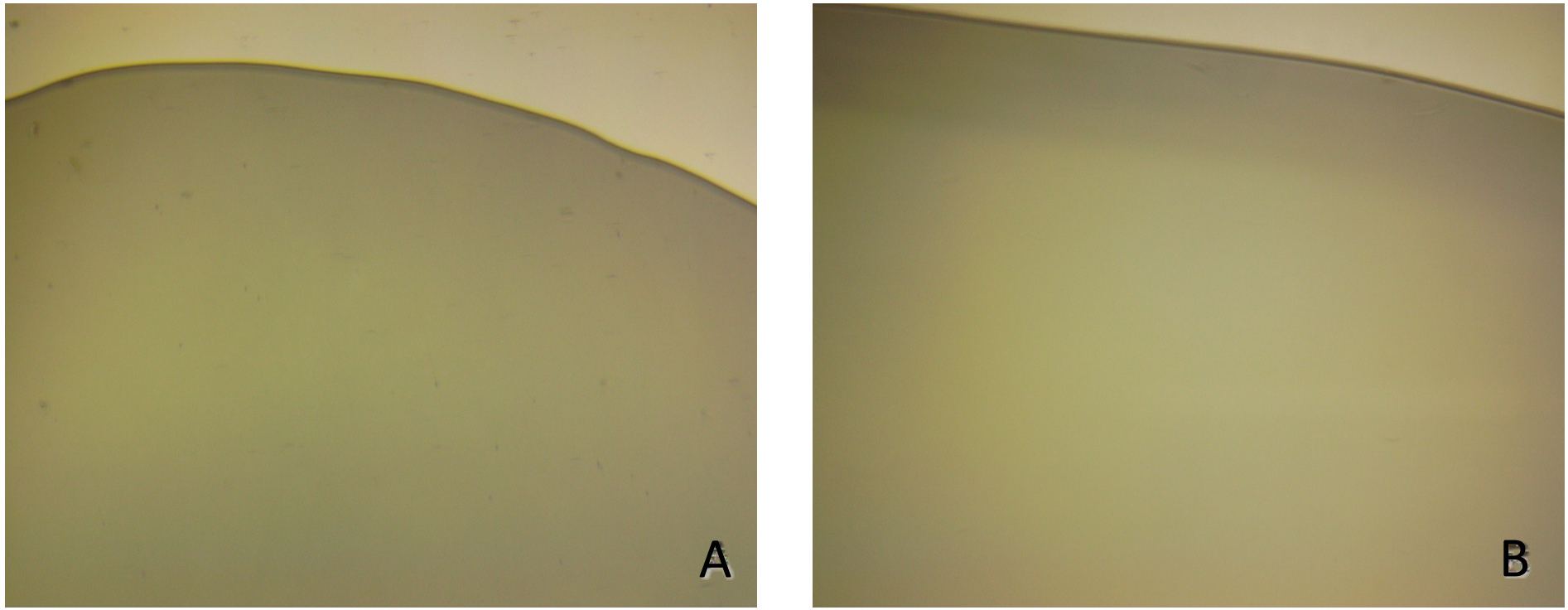

Fig S35: Microcrystalline cellulose not completely dissolved in **N_{8881}Lev/DMSO** (100 °C, 13 wt%), 4x(**A**) and 15x (**B**),

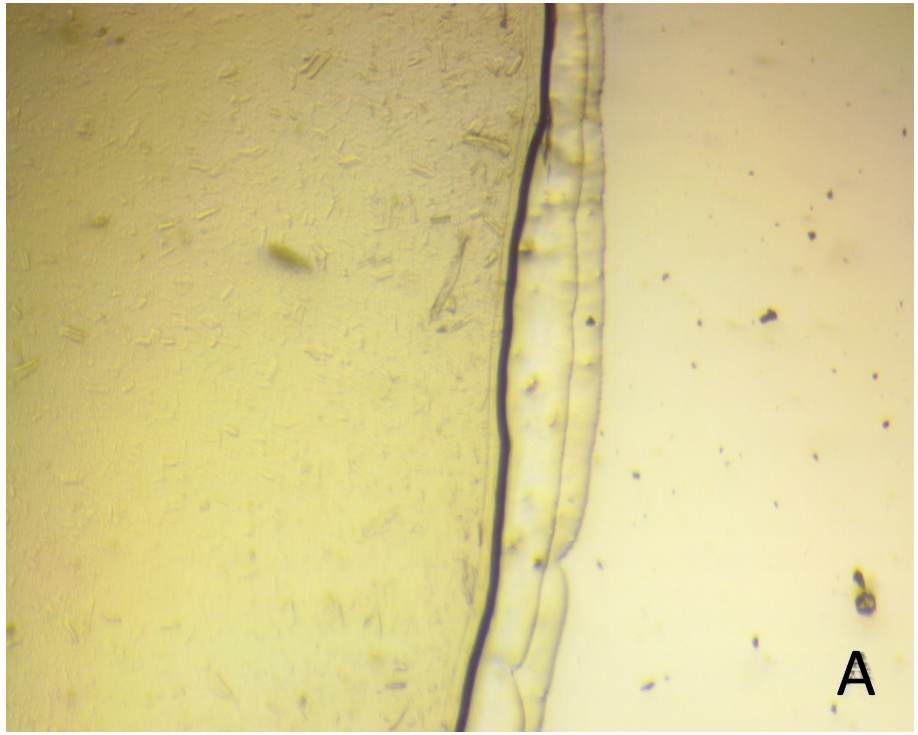

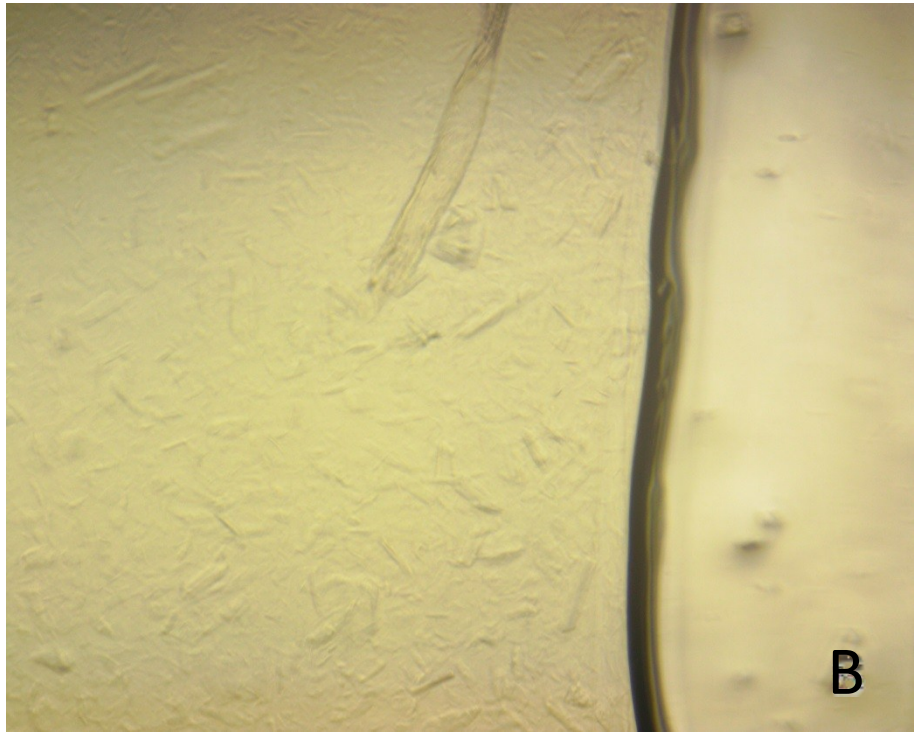

Fig S36: Optical microscopy of MCC dissolved in **P_{8881}Lev/DMSO** (100 °C, 10 wt%), 4x(**A**) and 15x (**B**)

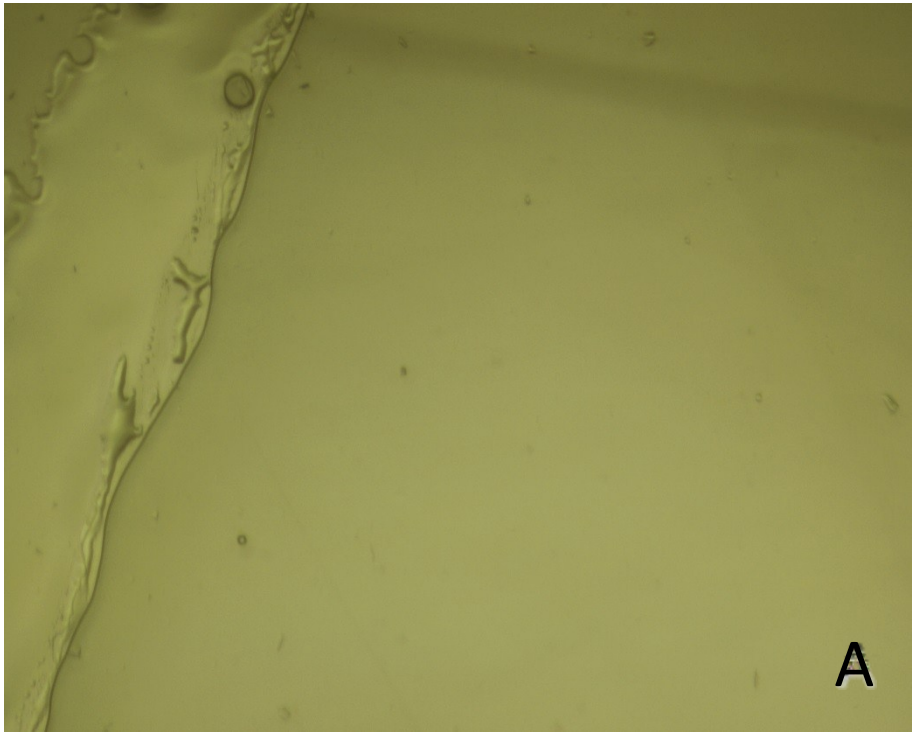

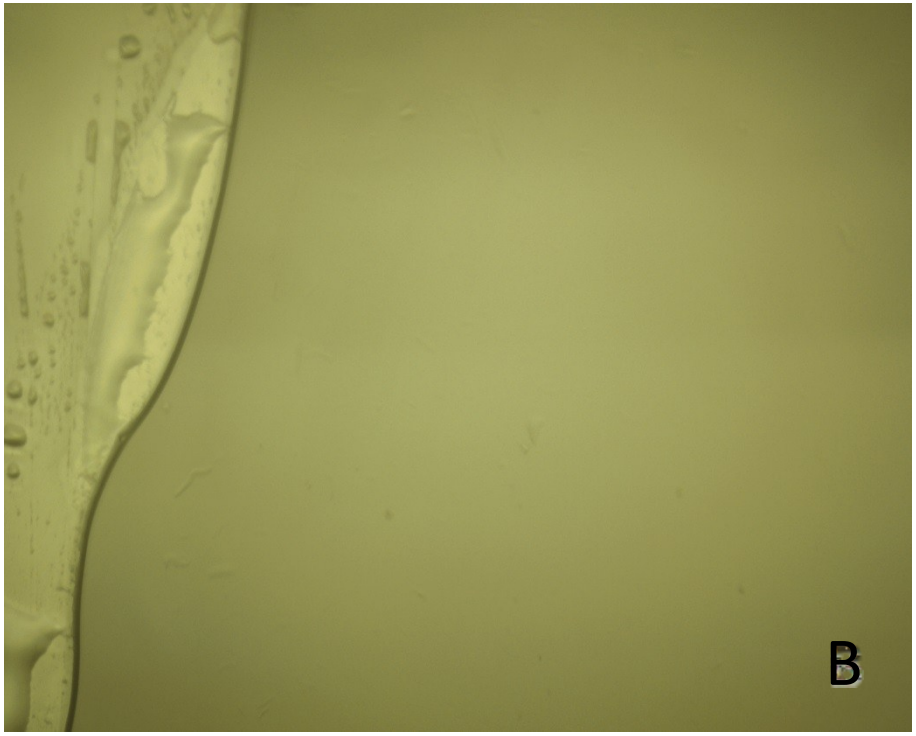

Fig S37: IR of MCC

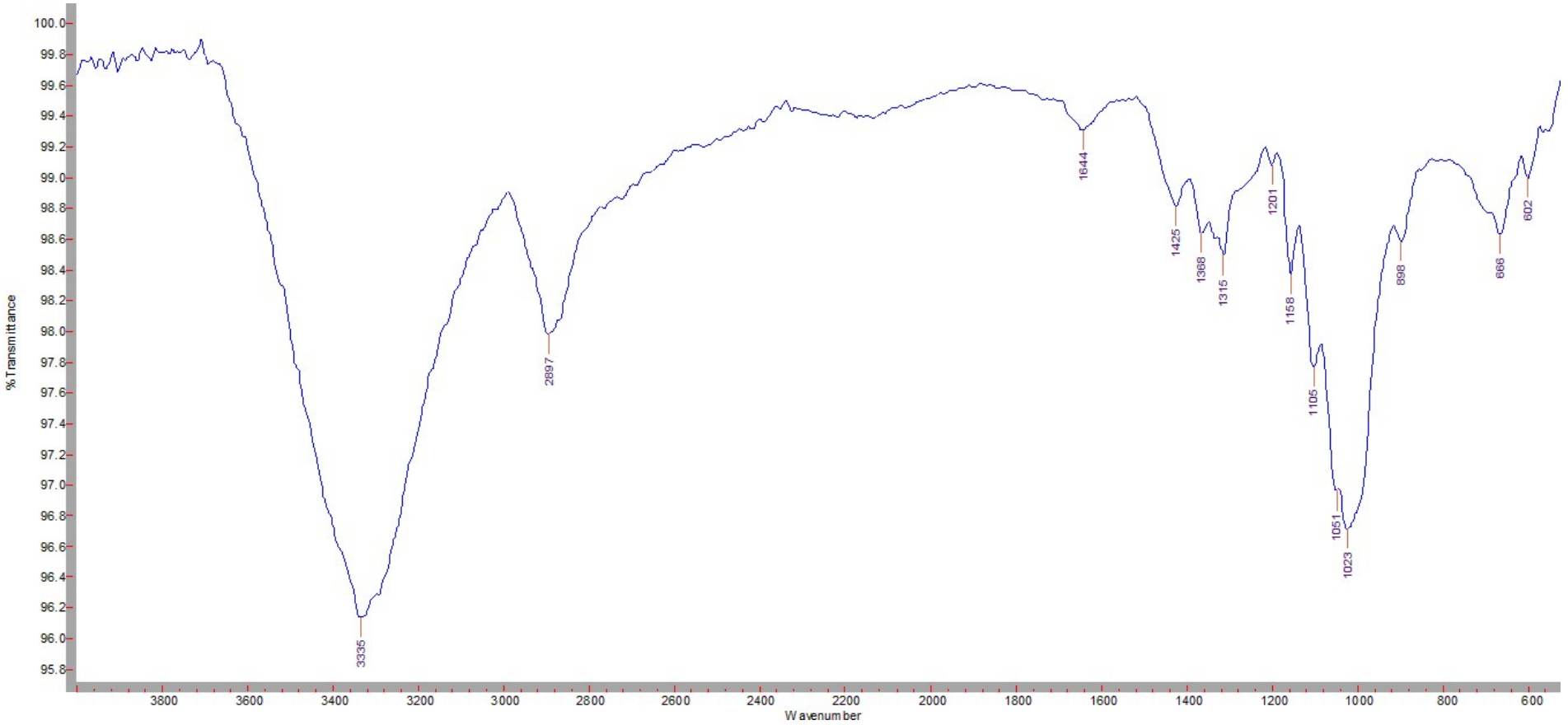

Fig S38: IR of regenerated cellulose after dissolution in **EMIMLev** at 100 °C

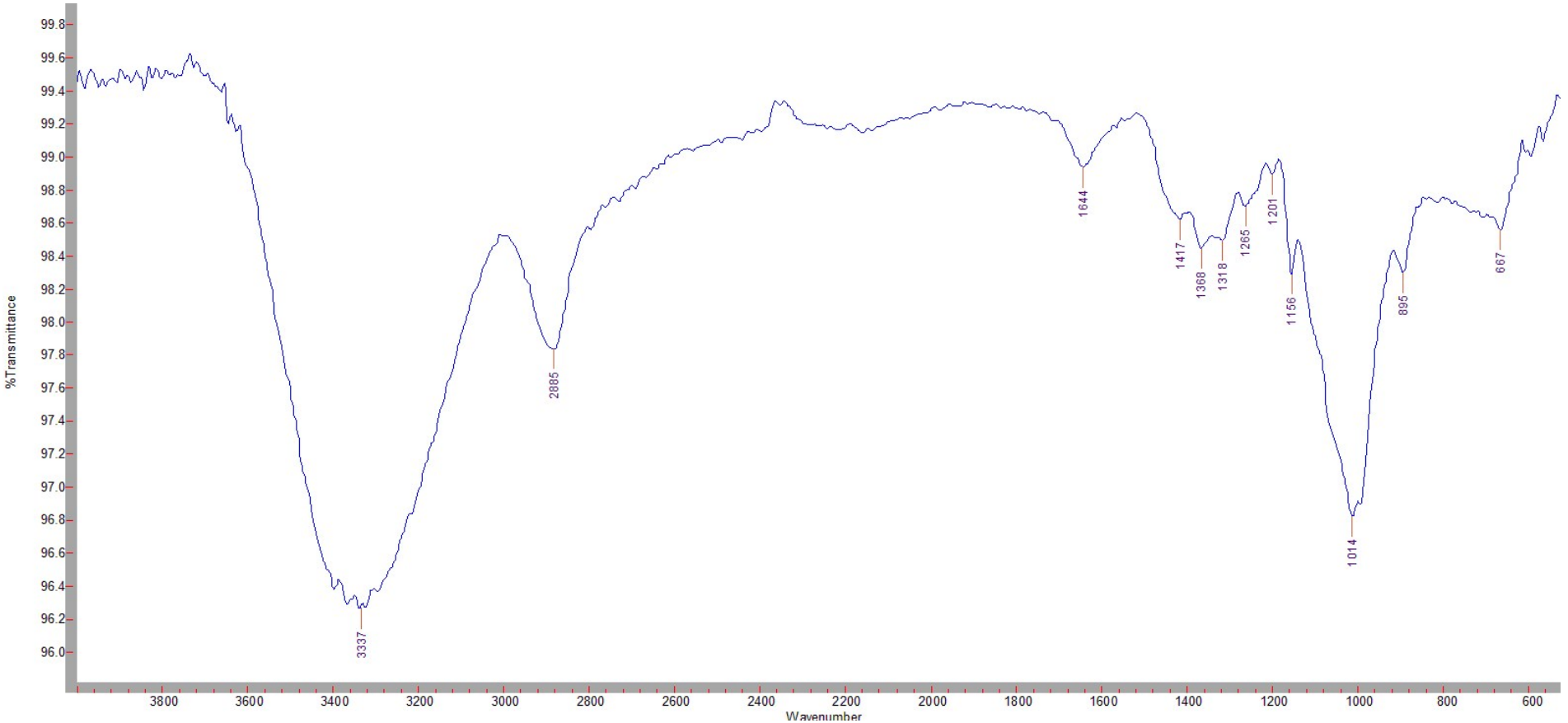

Fig S39: IR of regenerated cellulose after dissolution in **BMIMLev** at 100 °C

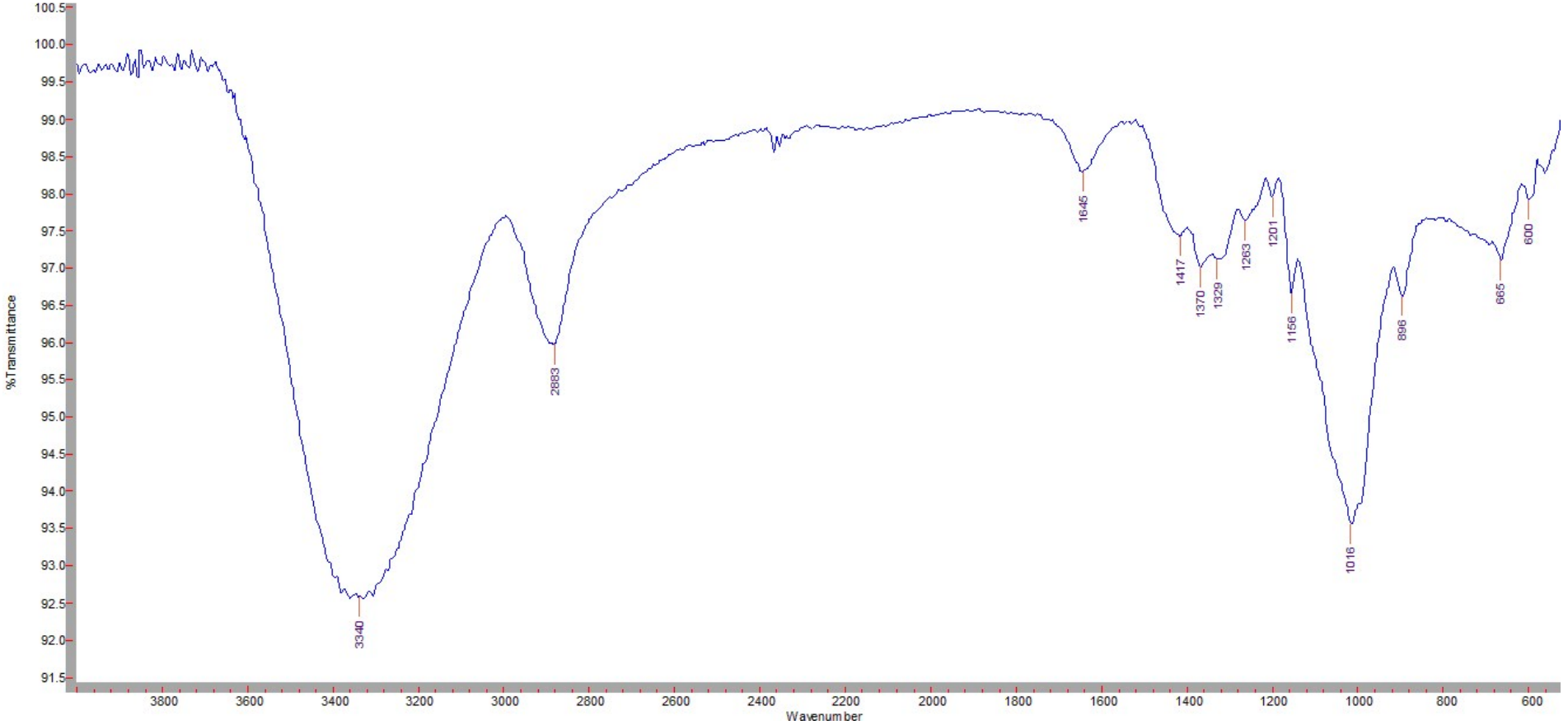

Fig S40: IR of regenerated cellulose after dissolution in **N_{8881}Lev/DMSO** at 100 °C

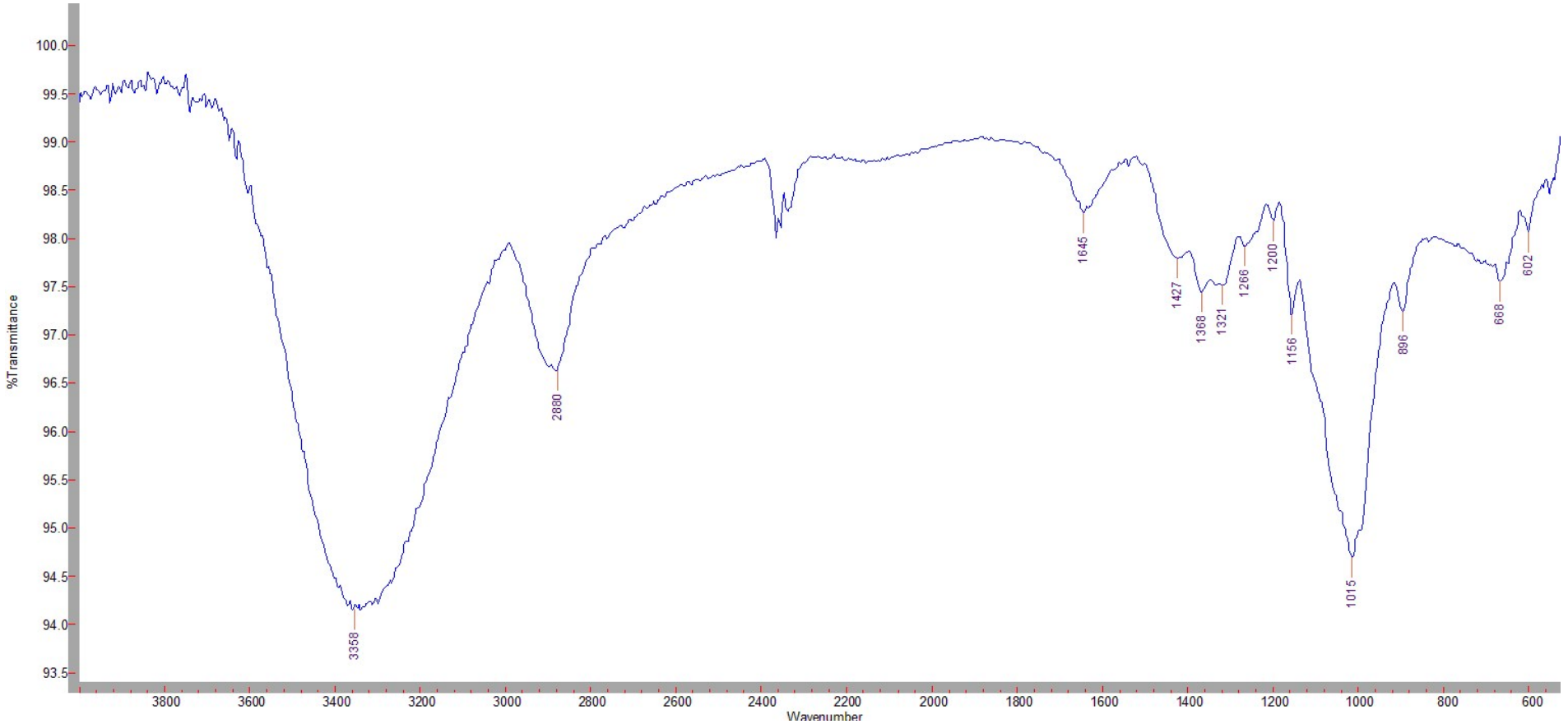

Fig S41: IR of regenerated cellulose after dissolution in **P_{8881}Lev/DMSO** at 100 °C

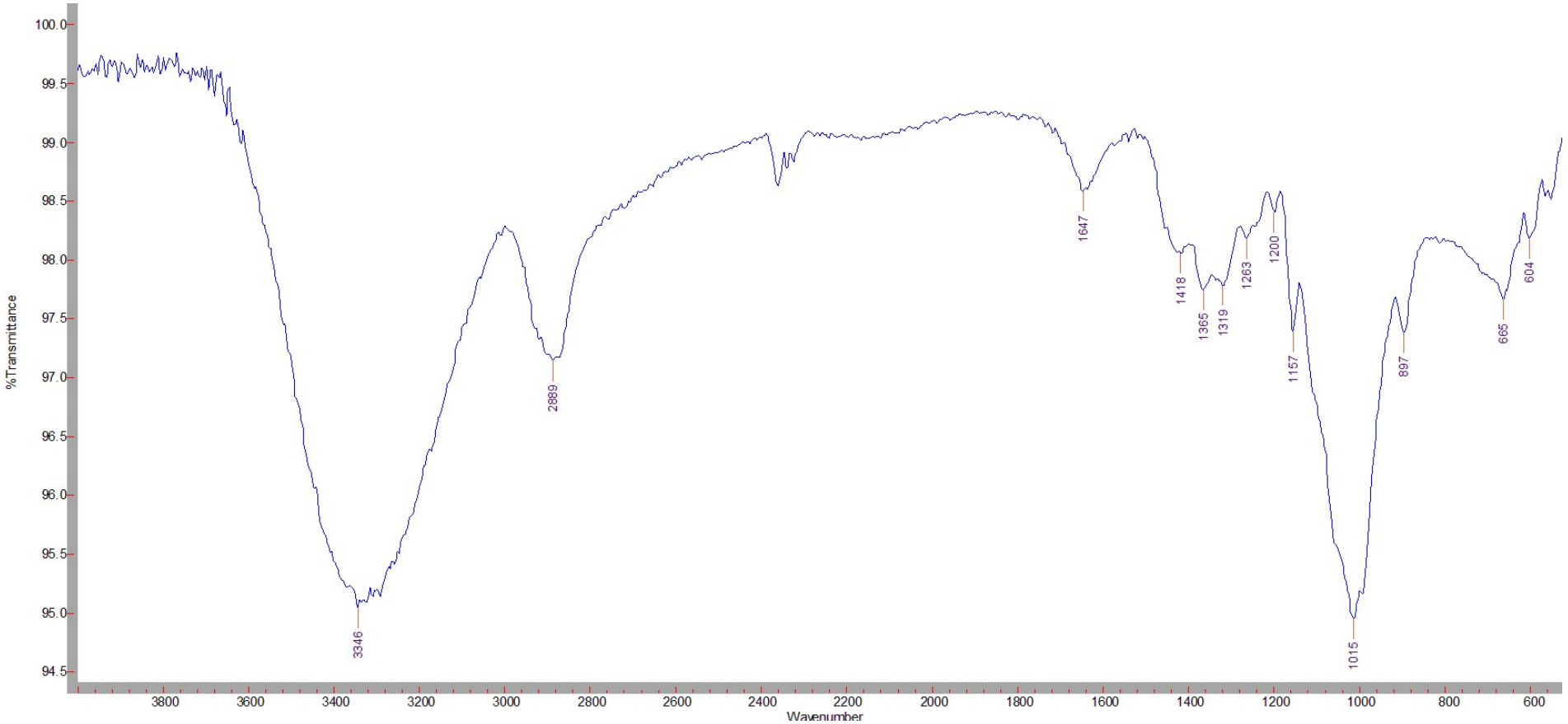

Fig S42: Interferograms of MCC and regenerated cellulose from [EMIM][Lev] at various temperatures